General conditions for intrinsic optical bistability at the atomic and molecular scale: An effective spin-Hamiltonian approach

O. Guillot-Noël,* L. Binet, and D. Gourier
Ecole Nationale Supérieure de Chimie de Paris (ENSCP), Laboratoire de Chimie Appliquée de l'Etat Solide, UMR-CNRS 7574, 11 rue Pierre et Marie Curie, 75231 Paris Cedex 05, France

(Received 20 April 2001; revised manuscript received 3 December 2001; published 28 May 2002)

A model for intrinsic optical bistability is presented in the case of systems that can be described as two weakly interacting subsystems embedded in a matrix M. This model is based on an effective spin-Hamiltonian and a semiclassical density-matrix approach. It is shown that optical bistability should occur when the interaction between the two subsystems fluctuates more rapidly than the characteristic time of the interaction. The validity of the model is demonstrated in the case of bistable electron magnetic resonance, involving real spins. It is also shown that this model provides a semiquantitative explanation of intrinsic optical bistability for Yb^{3+} pairs in $CsCdBr_3$ matrix.

DOI: 10.1103/PhysRevB.65.245101 PACS number(s): 71.10.Li, 42.65.Pc, 42.50.Md

I. INTRODUCTION

Research on systems exhibiting intrinsic optical bistability (IOB) has been motivated by the hope to replace electrons by photons in future data systems. Generally speaking, a system is bistable if it exhibits two stable output responses R for a single input signal or perturbation P. This property manifests itself by a hysteresis loop in the curve $R=f(P)$, which reveals a different response of the system for upward and downward sweep of the input signal. Two ingredients are required to generate a bistable phenomenon: (i) a feedback loop and (ii) a nonlinear process. In the cases studied earlier the systems consist of a nonlinear medium placed in a Fabry-Perot interferometer.[1] For such devices the bistability is macroscopic, whereby the nonlinearity is brought by the medium and the feedback loop is due to the cavity mirrors. More recently, active research has been initiated in the domain of mirrorless or IOB at the most elementary atomic scale. In this paper, by ''optical'' we mean the whole spectral range from microwave to visible light, but it is obvious that visible or infrared range is required for practical applications in telecommunication and data processing.

Up to now, there are only three systems in which IOB has been observed and understood, i.e., the bistability of the cyclotron resonance of a single electron in a Penning trap in InSb,[2] the bistable electron paramagnetic resonance (EPR) of shallow donor electrons in semiconductors and conduction electrons in metallic lithium,[3–5] and the bistable hysteresis of the optical absorption in CdS.[6] In the first system, the response R is the cyclotron kinetic energy and the perturbation P is the driving frequency, the feedback loop originating from the relativistic mass increase of the electron. In the second system, the response is the EPR intensity and the perturbation is the magnetic field or the microwave intensity. The feedback loop is due to ''flip-flop'' relaxation between electrons and nuclear spins inducing a nuclear polarization known as the Overhauser effect.[7] In the third system, the response R is the band-gap absorption coefficient and the perturbation P is the incident laser power, the feedback loop resulting from a reduction of the band gap produced by the excitation of the electron-hole plasma.

Recently, IOB has been observed for the near-infrared and for the visible cooperative luminescence of Yb^{3+} pairs in halide matrices: $Cs_3Y_2Br_9$,[8] $Cs_3Lu_2Br_9$,[9,10] $CsCdBr_3$,[10,11] and in the Yb^{3+}/Tm^{3+}-codoped glass system.[12] In these systems, the response is the rare-earth fluorescence and the perturbation is the incident laser power. However, the origin of the feedback loop is not yet understood. For most authors, the feedback loop is due to the so-called Lorentz local-field correction originating from interacting Yb^{3+} ions forming pairs.[8,9,11,12] This idea is based on the previous works of Bowden and co-workers,[13,14] Hopf and co-workers[15] Friedberg, Hartmann, and Manassah[16] Ben-Aryeh and co-workers,[17] Stroud, Bowden, and Allen,[18] Inguva and Bowden[19] and Crenshaw and co-workers.[20] They generally consider a collection of two-level atoms in vacuum,[13,15,16,18] or in a dielectric medium,[14,20] driven by an externally applied coherent field. The local-field correction, which gives the feedback loop, is due to a ground-state electric dipole-dipole interaction between these two-level atoms. A central atom absorbs the external field and induces a polarization of its nearest neighbors by interacting with the other atoms. In addition to the ground-state interaction, Hehlen *et al.* consider interactions between excited states of two ytterbium ions forming dimers, which take into account cooperative upconversion processes.[8] The role of this term is to enhance the bistability phenomenon. However, in a recent study, Gamelin, Lüthi, and Güdel propose that a completely different mechanism could be responsible for IOB in $Cs_3Lu_2Br_9:Yb^{3+}$ and $CsCdBr_3:Yb^{3+}$.[10] The bistability is explained as the result of laser heating effects and is expected to occur for isolated ions instead of pairs. It thus appears that the origin of the bistability in Yb^{3+}-doped halide matrices is still beyond discussions and the situation is far from being clear.

Parallel to these studies, a controversy appears concerning the occurrence of IOB in pairs of atoms. From Heber's work IOB can be expected for coupled ion pairs in solids.[21] The interactions between the two ions can be more general than the dipole-dipole interaction, and other mechanisms such as

exchange or superexchange have to be taken into account. Malyshev and co-workers suggest that the optical response of a dimer is a single-valued function and can never manifest a bistable behavior, only aggregates with a large number of ions can give a bistable optical response.[22,23]

In this work, we propose a treatment of IOB by an effective spin-Hamiltonian model. This kind of approach is commonly used in magnetic resonance to describe relaxation processes in spin systems (see Refs. 24 and 25, for example). However, the aim of the present work is to apply the effective spin approach to metal ions such as rare-earth ions or transition ions, and to discuss the conditions that a system has to fulfill to present a bistable behavior. The mechanism studied in this work can be described as follows. In a very general way, the system S under study is always composed of two subsystems L and K weakly interacting via an interaction V. These two subsystems can be embedded in a medium M. For example, in the case of the Lorentz local-field correction, the L system is the atom probed by the incident light, the K system consists of the nearest neighbors of this central atom, and V is the ground-state dipole-dipole interaction. In the case of a dimer, the two subsystems are the two ions of the pair and the interaction V can be of magnetic, exchange, or superexchange type. In a very schematic way, the total system S can be written as

$$S = L \otimes K + C^{LK}, \tag{1}$$

where C^{LK} represents the correlation terms between the two systems. By definition, the host M has several degrees of freedom and thus can be treated as a ''reservoir'' or a ''heat bath'' in a steady state. Two very different cases have to be considered for the time evolution of S under an external perturbation.

(i) The two weakly interacting subsystems cannot be distinguished experimentally and we cannot neglect the correlation terms between K and L. The measurements probe the total S system. Under steady-state conditions, the kinetic equations describing the evolution of S interacting with an external field give a single-valued solution for the response of the system. This case has been already discussed by Malyshev, Glaeske, and Feller,[22] and will not be studied in this work.

(ii) The two subsystems L and K can be distinguished experimentally. In this case, we can isolate one system and the interaction with the other system is taken into account via an average interaction. During the time scale of the evolution of L and K, the contribution of the correlation terms between these two subsystems is neglected, so that Eq. (1) becomes

$$S = L \otimes K. \tag{2}$$

We clearly demonstrate in this work that Eq. (2), hereafter referred to as the ''factorization operation,'' is based on the following condition:

$$\tau_c \ll \frac{\hbar}{V}, \tag{3}$$

where τ_c, the correlation time associated with the interaction V, measures the time during which the two subsystems retain the memory of their mutual interaction. This factorization has already been pointed out as a key step for bistable phenomenon by Hopf and co-workers[15] and Ben-Aryeh and co-workers.[17] However, the operation is always postulated without any justification,[17] or is explained in a heuristic manner, or justified by numerical simulations.[15] This condition is the origin of the controversy between Malyshev and co-workers[22] and Heber.[21] The first author discusses situations with $\tau_c \gg \hbar/V$, while Heber discusses situations with $\tau_c \ll \hbar/V$.

We show hereafter that when condition (3) is fulfilled, the response R of the system under steady-state conditions can be written with two coupled equations of the type

$$R = \frac{a}{1 + b(c-\omega)^2 + a}, \tag{4}$$

$$R = (d-\omega)\frac{1}{e}, \tag{5}$$

where ω is the angular frequency of the external applied field and coefficients $a-e$ are functions of control parameters such as the temperature and the power of the incident radiation, and of material-dependent parameters such as the frequency of the transition and the time relaxation terms of the system. Equations (4) and (5) correspond to the nonlinear process and the feedback loop, respectively [see Eqs. (40) and (41) in Sec. III A]. To get IOB, a renormalization of the resonance frequency of the transition is necessary. By renormalization, it is meant that the frequency of the transition has to change continuously during the interaction with the external field. In the paper, we show that this renormalization is included in Eq. (5), which directly comes from the factorization operation and, therefore, from the condition $\tau_c \ll \hbar/V$. All systems described by Eqs. (4) and (5) can exhibit a bistable behavior. Figure 1 is a graphical representation of the coupled equation (4) and (5). The system is monostable when the straight line of Eq. (5) and the bell-shaped curve of Eq. (4) have only one crossing point [Fig. 1(a), case (i)]. The system is bistable when there are three crossing points α, β, γ [Fig. 1(a), case (ii)] with two steady states α and γ and one unstable state β. Another way to represent this phenomenon is to plot the set of crossing points of these two equations, which represent the line shape of the transition [Fig. 1(b)]. In the monostable case, the response R of the system exhibits a symmetrical line shape without hysteresis. The response of the system is the same whether the frequency is swept upward or downward [case (i)], which is the general situation in spectroscopy. Under certain conditions, the theoretical line shape can be bent in such way as to describe a ''shark fin'' shape [Fig. 1(b) case (ii)]. In this case, with particular values of the $a-e$ parameters, the response R becomes dependent on the frequency sweep direction with a hysteresis window limited by abrupt transitions at $\omega^{\uparrow}$ and $\omega^{\downarrow}$ between the two steady states α and γ. When the frequency is swept upward, the system is on the α branch until $\omega^{\uparrow}$ and switches abruptly to the γ branch. When the frequency is swept downward the

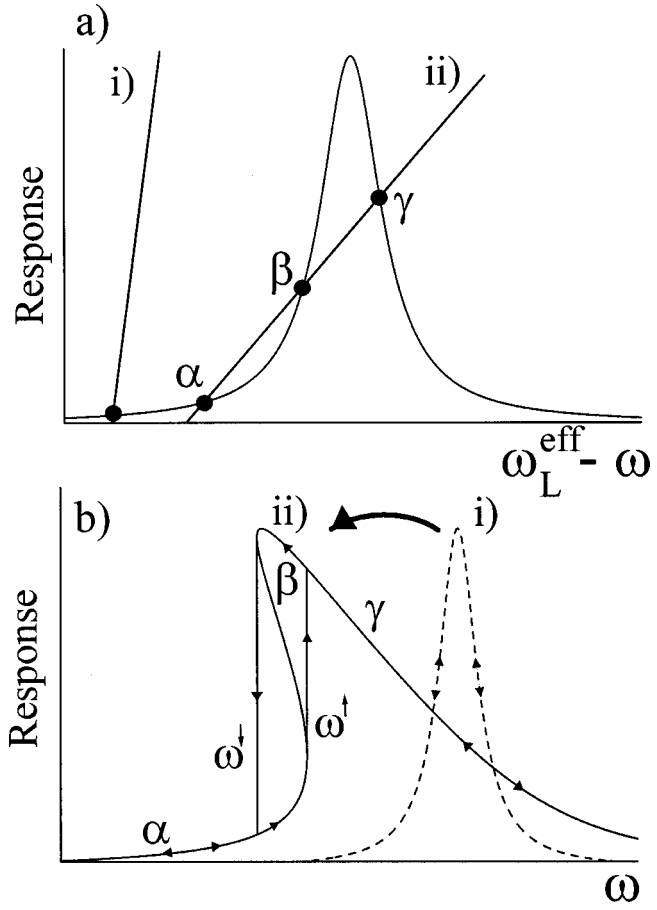

FIG. 1. (a) Graphical representation of the response R of the system [Eqs. (4) and (5)] versus the frequency ω of the external field. Case (i) corresponds to a monostable situation with one crossing point between the bell-shaped response [Eq. (4)] and the straight line [Eq. (5)]. Case (ii) corresponds to a bistable situation with three steady-state points (α, β, γ). (b) Principle of bistability and hysteresis of the response of the system induced by an external field. The monostable transition (i) and the bistable ''shark fin'' shape transition (ii) are represented by the discontinuous line and full line, respectively.

system is on the γ branch until $\omega^{\downarrow} \neq \omega^{\uparrow}$ and switches to the α branch. The unstable β branch cannot be recorded.

This paper is organized as follows. In Sec. II, we discuss the factorization operation and the approximations of the model. We present the spin-Hamiltonian approach, which leads to the kinetic equations representing the time evolution of the S system interacting with an external radiation field. Two situations are considered in which the two subsystems K and L are different or identical. This approach is based on a semiclassical density-matrix formalism. In Sec. III, the previous kinetic equations are solved under steady-state conditions. We obtain the coupled Eqs. (4) and (5) and a continuous shift of the frequency of the transition under study resulting from the factorization operation. We discuss the condition for the occurrence of IOB, and demonstrate that in order to obtain a bistable ''shark fin'' shape as shown in Fig. 1(b), that is, to obtain a bistability phenomenon, the maximum shift of the frequency must be larger than the homogeneous linewidth of the transition. Based on this criterion, we obtain a ''phase diagram'' for bistability ranging from the microwave domain up to the visible domain. The effects of the material-dependent parameters as well as the control parameters are discussed. In Sec. IV, we illustrate the previous model in the microwave range for the case of bistable magnetic resonance of electrons in semiconductors such as β-Ga_2O_3 or InP and in metallic Li. This well-understood example of IOB validates all the required conditions discussed in Sec. II. In a second part, the phase diagram is used to discuss the possibility of a bistability in the infrared and visible range in the particular case of ytterbium ion pairs. We show that the effective spin approach can qualitatively explain with a correct order of magnitude all the previous results obtained in the $CsCdBr_3:Yb^{3+}$ system.

II. SPIN-HAMILTONIAN APPROACH

A. Position of the problem

Let us consider a system S composed of two weakly interacting subsystems K and L connected by an interaction V and embedded in a medium M. The two subsystems K and L can be, for example, two different or identical ions, or a cluster of ions characterized by a complex energy-level diagram. An effective spin **K** and **L** is associated to each subsystem. As we focus on a particular transition by applying an electromagnetic field of angular frequency ω close to the resonance frequency of the transition, the two levels connected by the field can be described by an effective spin $\frac{1}{2}$. The contribution of the other levels to the evolution of the system is taken into account via phenomenological relaxation terms. In the following, we consider only an interaction between two single ions; however all the results can be easily generalized to larger clusters of interacting atoms or ions.

The effective spin-Hamiltonian of the S system in the lattice M is written as

$$H = H_L + H_K + H_M + V, \tag{6}$$

where $H_L = \hbar \omega_L L_z$ and $H_K = \hbar \omega_K K_z$ are the effective spin Hamiltonians associated with the isolated two-level systems L and K, respectively, with $\hbar \omega_L$ and $\hbar \omega_K$ being the corresponding energy splittings. H_M is the energy operator describing the lattice. By definition, the interaction V between K and L is Hermitian and is written in a very general way as

$$V = \sum_p \left(F_p S^{(p)} + F_p^* S^{(p+)}\right), \tag{7}$$

where F_p are constants that represent the interaction and $S^{(p)}$ are products of two operators associated with the two subsystems. The sign + means the adjoint operator and * represents the complex conjugate. Equation (7) can be expanded as follows:

$$V = F_0 L_z K_z + F_1 L_+ K_- + F_1^* L_- K_+ + F_2 L_+ K_z + F_2^* L_- K_z + F_3 L_z K_+ + F_3^* L_z K_- + F_4 L_+ K_+ + F_4^* L_- K_-, \tag{8}$$

where $L_{z,\pm}$ and $K_{z,\pm}$ are effective spin operators. For example, in the case of a scalar interaction A, Eq. (8) reads V

$=AL_zK_z+(A/2)(L_+K_-+L_-K_+)$. For a dipole-dipole type interaction, see Refs. 24 and 25.

$T_{1,2}^{L^{\text{int}}}$ and $T_{1,2}^{K^{\text{int}}}$ represent the longitudinal (subscript 1) and transverse (subscript 2) relaxation terms due to the interaction V and associated with L and K, respectively, and $T_{1,2}^{L^{\text{other}}}$ and $T_{1,2}^{K^{\text{other}}}$ represent the longitudinal and transverse relaxation terms due to all the other mechanisms. These terms can be due to stimulated or spontaneous emission, and take into account the phenomenological relaxation terms resulting from the complex energy-level diagram of each subsystem. τ_c denotes the correlation time associated with V. K and L are correlated for $\tau \ll \tau_c$, and the two subsystems become progressively less correlated when τ increases until $\tau \gg \tau_c$, where the correlations vanish. τ_c is thus a measure of the time during which the two subsystems retain the ''memory'' of their mutual interaction.

The density operator ρ of the whole system is written in the form

$$\rho(t)=\sigma^K(t)\otimes\sigma^L(t)\otimes\sigma^M(t)+\rho^{KL}(t)+\rho^{LM}(t)+\rho^{KM}(t), \tag{9}$$

where $\sigma^K(t)$, $\sigma^L(t)$, and $\sigma^M(t)$ are the reduced density-matrix operators of the K, L, and M systems, respectively. They are obtained from ρ by taking the trace over all the variables of L and M, K and M, and L and K, respectively, i.e., $\sigma^K=\mathrm{Tr}_{LM}(\rho)$, $\sigma^L=\mathrm{Tr}_{KM}(\rho)$, and $\sigma^M=\mathrm{Tr}_{LK}(\rho)$. The other terms ρ^{KL}, ρ^{LM}, and ρ^{KM} of Eq. (9) are the correlations terms between K and L, L and M, and K and M, respectively. In the following, $\sigma^S(t)$ denotes the density operator of the S system given by $\sigma^S(t)=\sigma^K(t)\otimes\sigma^L(t)+\rho^{KL}(t)$. The time evolution of S is obtained by solving the von Neumann equation

$$\frac{d}{dt}\rho(t)=\frac{1}{i\hbar}[H,\rho(t)]. \tag{10}$$

Two cases have to be considered. In the first one, the interaction V does not fluctuate, which corresponds to $\tau_c \gg \hbar/V$. The two subsystems L and K cannot be distinguished and the total system $S=L+K$ must be studied. The V interaction is time independent and gives a multiplet structure in the energy-level diagram of S. For example, this case is commonly encountered in electron paramagnetic resonance spectroscopy with hyperfine interactions between an electron spin and a nuclear spin. Under the condition $\tau_c \gg \hbar/V$, the contribution of the correlation terms between L and K cannot be neglected in Eq. (9) and the total density-matrix operator ρ must be worked out. We will not discuss this case further, see Ref. 22 for more details. In the second case, the interaction V fluctuates faster than $\hbar/V$ that is $\tau_c \ll \hbar/V$. It means that the multiplet structure resulting from V disappears and each subsystem feels an average interaction V.[24] One of the two subsystems can be probed independently of the other that is left undetected. The undetected system influences the measured one via a mean field proportional to V. Under this condition, V becomes another relaxation mechanism for the two subsystems L and K, which can be included and associated with the host M. The F_p terms of Eqs. (7) and (8) become fluctuating functions of time characteristic of the medium, and V can be written as

$$V(t)=\sum_p [F_p(t)S^{(p)}+F_p^*(t)S^{(p+)}]. \tag{11}$$

In the following (Sec. II B), we show that the condition $\tau_c \ll \hbar/V$ is equivalent to $\tau_c \ll T_{1,2}^{L^{\text{int}}}$, $T_{1,2}^{K^{\text{int}}}$. If Eq. (10) is integrated between t and $t+\Delta t$ with $\tau_c \ll \Delta t \ll T_{1,2}^{L^{\text{int}}}$, $T_{1,2}^{K^{\text{int}}}$, the calculation can be limited to second order in the perturbation and the contribution of the correlation terms to Eq. (9) can be neglected. It means that we can write in this case

$$\rho(t)=\sigma^K(t)\otimes\sigma^L(t)\otimes\sigma^M(t), \tag{12}$$

$$\sigma^S(t)=\sigma^K(t)\otimes\sigma^L(t).$$

This factorization operation is at the origin of the so-called renormalization of the resonance frequency. This is the situation studied in this work. Rewritten in the interaction picture, Eq. (10) becomes

$$\frac{d}{dt}\tilde{\rho}(t)=\frac{1}{i\hbar}[\tilde{V}(t),\tilde{\rho}(t)], \tag{13}$$

where

$$\tilde{\rho}(t)=e^{i(H_L+H_K+H_M)t/\hbar}\rho(t)e^{-i(H_L+H_K+H_M)t/\hbar},$$

$$\tilde{V}(t)=e^{i(H_L+H_K+H_M)t/\hbar}V(t)e^{-i(H_L+H_K+H_M)t/\hbar},$$

$$\tilde{S}^{(p)}(t)=e^{i(H_L+H_K)t/\hbar}S^{(p)}e^{-i(H_L+H_K)t/\hbar}.$$

By integrating Eq. (13) from t to $t+\Delta t$ and taking the trace over all the variables of the host M, we obtain

$$\Delta\tilde{\sigma}^S(t)=\tilde{\sigma}^S(t+\Delta t)-\tilde{\sigma}^S(t)=\frac{1}{i\hbar}\int_t^{t+\Delta t}dt'\,\mathrm{Tr}_M[\tilde{V}(t'),\tilde{\rho}(t)]$$
$$+\left(\frac{1}{i\hbar}\right)^2\int_t^{t+\Delta t}dt'\int_t^{t'}dt''\,\mathrm{Tr}_M[\tilde{V}(t'),[\tilde{V}(t''),\tilde{\rho}(t'')]]. \tag{14}$$

Under the condition $\tau_c \ll \hbar/V$, the interaction V is incorporated in the host and behaves as another relaxation mechanism. Since M, by definition, possesses many degrees of freedom, it quickly dissipates the effects of the interaction. This means that the medium M can be considered in a stationary state and is constant in the interaction picture:

$$\tilde{\sigma}^M(t)=\tilde{\sigma}^M(0)=\sigma^M. \tag{15}$$

As $|V| \ll |H_K|$, $|H_L|$, $|H_M|$, the density operator $\tilde{\rho}(t)$ does not vary significantly between t and t'' for an integration time $\Delta t \ll T_{1,2}^{L^{\text{int}}}$, $T_{1,2}^{K^{\text{int}}}$. We can, therefore, substitute $\tilde{\rho}(t'')$ by $\tilde{\rho}(t)$ in the second integral of Eq. (14). This approximation is equivalent to stop the calculation up to second order in perturbation. $\tilde{\rho}(t)$ depends only on its present value and loses the memory of its past, which is the well-known Markoff

approximation. The double commutator in the second integral of Eq. (14) is proportional to the time correlation function $\langle \tilde{V}(t')\tilde{V}(t'')\rangle_M = \mathrm{Tr}_M[\tilde{\sigma}^M \tilde{V}(t')\tilde{V}(t'')]$. This function characterizes the correlations between the interactions at times t' and t''. Since M quickly dissipates the effect of the interaction, the time correlation function vanishes for $\tau = t' - t'' \gg \tau_c$. Therefore, for an integrating time $\Delta t \gg \tau_c$, the correlations do not contribute to Eq. (14) and then $\tilde{\rho}^{KL}(t)$, $\tilde{\rho}^{LM}(t)$, and $\tilde{\rho}^{KM}(t)$ can be neglected. Taking into account Eq. (15) and the inequality $\tau_c \ll \Delta t \ll T_{1,2}^{L^{\mathrm{int}}}$, $T_{1,2}^{K^{\mathrm{int}}}$, Equation (14) becomes

$$\Delta\tilde{\sigma}^S(t) = \frac{1}{i\hbar}\int_t^{t+\Delta t} dt' \mathrm{Tr}_M[\tilde{V}(t'), \tilde{\sigma}^K(t)\otimes\tilde{\sigma}^L(t)\otimes\tilde{\sigma}^M] + \left(\frac{1}{i\hbar}\right)^2 \int_t^{t+\Delta t} dt' \int_t^{t'} dt'' \mathrm{Tr}_M[\tilde{V}(t'),[\tilde{V}(t''),\tilde{\sigma}^K(t) \otimes \tilde{\sigma}^L(t)\otimes\sigma^M]]. \quad (16)$$

If we introduce $\tau = t' - t''$, we can replace $\int_t^{t+\Delta t} dt' \int_t^{t'} dt''$ by $\int_0^{\Delta t} d\tau \int_{t+\tau}^{t+\Delta t} dt'$ so that Eq. (16) can be written as[26,27]

$$\frac{\Delta\tilde{\sigma}^S(t)}{\Delta t} = \frac{1}{i\hbar}\frac{1}{\Delta t}\int_t^{t+\Delta t} dt' \mathrm{Tr}_M[\tilde{V}(t'), \tilde{\sigma}^K(t)\otimes\tilde{\sigma}^L(t)\otimes\tilde{\sigma}^M] - \frac{1}{\hbar^2}\frac{1}{\Delta t}\int_0^{\Delta t} d\tau \int_{t+\tau}^{t+\Delta t} dt' \mathrm{Tr}_M[\tilde{V}(t'), [\tilde{V}(t'-\tau), \tilde{\sigma}^K(t)\otimes\tilde{\sigma}^L(t)\otimes\tilde{\sigma}^M]]. \quad (17)$$

As $\tau_c \ll \Delta t$ and $\langle \tilde{V}(t')\tilde{V}(t'')\rangle_M = 0$ for $\tau \gg \tau_c$, we set the upper limit of integration on τ at $+\infty$, and at t the lower limit of integration on t' so that we may replace $\int_0^{\Delta t} d\tau \int_{t+\tau}^{t+\Delta t} dt'$ by $\int_0^{+\infty} d\tau \int_t^{t+\Delta t} dt'$. Finally Eq. (17) becomes

$$\frac{\Delta\tilde{\sigma}^S(t)}{\Delta t} = \frac{1}{i\hbar}\frac{1}{\Delta t}\int_t^{t+\Delta t} dt' \mathrm{Tr}_M[\tilde{V}(t'), \tilde{\sigma}^K(t)\otimes\tilde{\sigma}^L(t)\otimes\tilde{\sigma}^M] - \frac{1}{\hbar^2}\frac{1}{\Delta t}\int_0^{+\infty} d\tau \int_t^{t+\Delta t} dt' \mathrm{Tr}_M[\tilde{V}(t'), [\tilde{V}(t'-\tau), \tilde{\sigma}^K(t)\otimes\tilde{\sigma}^L(t)\otimes\tilde{\sigma}^M]]. \quad (18)$$

B. Validity of the factorization operation

We analyze in this section the validity of the factorization operation by giving the order of magnitude of all the terms that are neglected in Eq. (18). The discussion is based on the treatment done for the case of a small system in interaction with a reservoir in Ref. 26. It is important to notice that this discussion is valid for only weak interactions V compared to the frequency of the transition. The two important approximations, namely, (i) the calculation limited to second order in perturbation and (ii) the factorization of the density operator $\rho(t) = \sigma^K(t)\otimes\sigma^L(t)\otimes\sigma^M$ can be checked by considering the order of magnitude of $T_{1,2}^{L^{\mathrm{int}}}$, $T_{1,2}^{K^{\mathrm{int}}}$.

Since $\langle \tilde{V}(t')\tilde{V}(t'')\rangle_M = 0$ for $\tau = t' - t'' \gg \tau_c$, the second integral can be restricted to an area $\tau_c \Delta t$ and Eq. (18) gives

$$\frac{\Delta\tilde{\sigma}^S(t)}{\Delta t} \sim \frac{1}{i\hbar} V\tilde{\sigma}^S(t) - \frac{1}{T_{1,2}^{L,K^{\mathrm{int}}}}\tilde{\sigma}^S(t) \quad (19)$$

with

$$\frac{1}{T_{1,2}^{L,K^{\mathrm{int}}}} = \frac{V^2\tau_c}{\hbar^2}. \quad (20)$$

Equation (20) and the condition $\tau_c \ll \hbar/V$ give $\tau_c \ll T_{1,2}^{L,K^{\mathrm{int}}}$ and $V\tau_c/\hbar \ll 1$. It is important to notice that in absence of fluctuations, we obtain $1/T_{1,2}^{L,K^{\mathrm{int}}} \sim V/\hbar$. Under the condition $\tau_c \ll \hbar/V$, the relaxation rates $1/T_{1,2}^{L,K^{\mathrm{int}}}$ are shortened by a factor $V\tau_c/\hbar \ll 1$. Since the homogeneous linewidth of the transition is proportional to $1/T_2^{L,K^{\mathrm{int}}}$, the condition $\tau_c \ll \hbar/V$ can be referred to as a narrowing condition.

The second-order calculation and the factorization operation can be justified by an estimation of the order of magnitude of the contribution of the third-order terms and of the correlation terms to Eq. (14), respectively.

The third-order terms are of the order of $(1/T_{1,2}^{L,K^{\mathrm{int}}}) \times (V\tau_c/\hbar)$. The inequality $V\tau_c/\hbar \ll 1$ gives $(1/T_{1,2}^{L,K^{\mathrm{int}}}) \times (V\tau_c/\hbar) \ll 1/T_{1,2}^{L,K^{\mathrm{int}}}$, which justifies to limit the calculation up to second order in perturbation as the third-order term are negligible compared to $1/T_{1,2}^{L,K^{\mathrm{int}}}$.

If we suppose $\rho^{KL}(t)$, $\rho^{LM}(t)$, $\rho^{KM}(t) \neq 0$ at time t, the correlation terms bring two contributions to Eq. (19).

(1) A *first-order* contribution. As the correlations between the two subsystems disappear for $\tau \gg \tau_c$, the order of magnitude of such terms is $V\tau_c/\Delta t$. Under the condition $\tau_c \ll \Delta t$, we have $V\tau_c/\Delta t \ll V$, these terms are thus negligible compared to V in Eq. (19).

(2) A *second-order* contribution. As $\rho^{KL}(t)$, $\rho^{LM}(t)$, $\rho^{KM}(t) \neq 0$ at time t, these terms result from an interaction before time t between the two subsystems L and K. Therefore, they bring a second-order contribution to $\Delta\tilde{\sigma}^S(t)/\Delta t$, which is due to an interaction before time t and to an interaction between t and $t+\Delta t$ and which can be written as $-(1/\hbar^2)(1/\Delta t)\int_{-\infty}^{t} dt' \int_t^{t+\Delta t} dt'' \langle \tilde{V}(t')\tilde{V}(t'')\rangle_M \tilde{\sigma}^S(t)$.[26] As the time correlation function $\langle \tilde{V}(t')\tilde{V}(t'')\rangle_M$ vanishes for $\tau \gg \tau_c$, these terms are of the order of $(1/T_{1,2}^{L,K^{\mathrm{int}}})(\tau_c/\Delta t)$. Under the condition $\tau_c \ll \Delta t$, we have $(1/T_{1,2}^{L,K^{\mathrm{int}}})(\tau_c/\Delta t) \ll 1/T_{1,2}^{L,K^{\mathrm{int}}}$. Therefore, the second-order contributions of the correlations terms are negligible compared to $1/T_{1,2}^{L,K^{\mathrm{int}}}$ in Eq. (19).

Finally, for $\tau_c \ll \Delta t$, the factorization of $\rho(t)$ is valid and the contributions of the correlation terms in Eq. (14) can be neglected. Equation (18) is obtained for an integration time Δt that fulfills the inequality $\tau_c \ll \Delta t \ll T_{1,2}^{L^{\mathrm{int}}}$, $T_{1,2}^{K^{\mathrm{int}}}$. The conditions $\tau_c \ll \Delta t$ and $\Delta t \ll T_{1,2}^{L^{\mathrm{int}}}$, $T_{1,2}^{K^{\mathrm{int}}}$ justify the factorization operation and the calculation up to second order in perturba-

tion, respectively. These simplifications are only due to the fundamental condition $\tau_c \ll \hbar/V$, which is equivalent to $\tau_c \ll T_{1,2}^{L,K^{\text{int}}}$.

Considering the left-hand side $\Delta\tilde{\sigma}^S(t)/\Delta t$ of Eq. (18), which is equal to $[\tilde{\sigma}^S(t+\Delta t)-\tilde{\sigma}^S(t)]/\Delta t$, if we assume $\tau_c \ll \Delta t$, but with Δt sufficiently small so that the changes in $\tilde{\sigma}^S(t)$ are linear in Δt, we can replace $\Delta\tilde{\sigma}^S(t)/\Delta t$ by the time derivative $d\tilde{\sigma}^S(t)/dt$. It is important to realize that the above kinetic equations cannot be use to describe changes of $\tilde{\sigma}^S(t)$ over time intervals shorter than τ_c.

C. Kinetic equations of the *S* system

After some calculations, Eq. (18) rewritten in the Schrödinger picture becomes

$$\frac{d\sigma^S(t)}{dt} = \frac{1}{i\hbar}\Bigg[H_K + H_L + \sum_p \left(\langle F_p\rangle S^{(p)} + \langle F_p^*\rangle S^{(p^+)}\right), \sigma^K(t) \otimes \sigma^L(t)\Bigg] - \frac{1}{\hbar^2}\sum_{p,q}\int_0^{+\infty} d\tau \langle F^p(t)F^q(t+\tau)\rangle e^{-i\omega^{S(q)}\tau}[S^{(p)}, S^{(q)}\{\sigma^K(t)\otimes\sigma^L(t)\}] - \frac{1}{\hbar^2}\sum_{p,q}\int_0^{+\infty} d\tau \langle F^q(t)F^p(t+\tau)\rangle \times e^{-i\omega^{S(q)}\tau}[\{\sigma^K(t)\otimes\sigma^L(t)\}S^{(q)}, S^{(p)}], \tag{21}$$

where $\langle F^p(t)F^q(t+\tau)\rangle$ are the time correlation functions and $\omega^{S^{(q)}}$ are the eigenvalues associated with the $S^{(q)}$ operator. Only the secular terms are kept in Eq. (21). For most types of interaction V, only the $\langle F^p(t)F^{p^+}(t+\tau)\rangle$ terms contribute to Eq. (21).[24] Under the Markoff approximation, the time correlation functions, which are real and even functions of τ, can be written as follows:[28]

$$\langle F^p(t)F^{p^+}(t+\tau)\rangle = \langle |F^p(0)|^2\rangle e^{-|\tau|/\tau_c}. \tag{22}$$

Combining Eqs. (21) and (22) gives

$$\frac{d\sigma^S(t)}{dt} = \frac{1}{i\hbar}\Bigg[H_K + H_L + \sum_p \left(\langle F_p\rangle S^{(p)} + \langle F_p^*\rangle S^{(p^+)}\right), \sigma^K(t) \otimes \sigma^L(t)\Bigg] - \frac{1}{2\hbar^2}\sum_p J_{pp^+}(\omega^{S^{(p)}})[S^{(p)}, [S^{(p^+)}, \sigma^K(t) \otimes \sigma^L(t) - \{\sigma^K(t)\otimes\sigma^L(t)\}^0]], \tag{23}$$

where we have neglected imaginary terms responsible for a second-order shift of the resonance, which are too weak to be detected experimentally in most cases.[24] The spectral density terms $J_{pp^+}(\omega^{S^{(p)}})$ in Eq. (23) are the Fourier transform of the time correlation functions and are given by

$$J_{pp^+}(\omega^{S^{(p)}}) = \langle |F^p|^2\rangle \frac{2\tau_c}{1+\omega^{S^{(p)2}}\tau_c^2}. \tag{24}$$

These terms are proportional to $1/T_{1,2}^{L,K^{\text{int}}}$ and, in particular, are related to the linewidth of the transitions. The term $[\sigma^K(t)\otimes\sigma^L(t)]^0$ in Eq. (23) is the density operator of the system S at thermal equilibrium.[24]

Experimentally, we have access to the macroscopic quantum-mechanical average $\langle Q\rangle$ of an operator Q. If Q is acting on the L system then $\langle Q\rangle = \mathrm{Tr}_L(\sigma^L Q)$ and the kinetic equation associated to this operator is

$$\frac{d\langle Q\rangle}{dt} = -\frac{1}{i\hbar}\left\langle\left[H_K + H_L + \sum_p \left(\langle F_p\rangle S^{(p)} + \langle F_p^*\rangle S^{(p^+)}\right), Q\right]\right\rangle - \frac{1}{2\hbar^2}\sum_p J_{pp^+}(\omega^{S^{(p)}})\langle[S^{(p^+)}, [S^{(p)}, Q - Q^0]]\rangle. \tag{25}$$

It is important to note that the term $\sum_p(\langle F_p\rangle S^{(p)} + \langle F_p^*\rangle S^{(p^+)})$ induces a shift in the resonance frequency of the system, which is the so-called renormalization of the resonance frequency. It comes from the factorization operation of the total density operator discussed in Sec. II B. In the following, we will focus on the quantum-mechanical average of the L_z, K_z and L_+, K_+ operators, which are, respectively, linked to the population inversion between the two levels under study and to the off-diagonal element of the density matrix by the following expressions:

$$\langle L_z\rangle = \tfrac{1}{2}(\sigma_{bb}^L - \sigma_{aa}^L), \tag{26}$$

$$\langle L_+\rangle = \sigma_{ab}^L, \tag{27}$$

where the subscripts a and b refer to the ground and excited states, respectively. $\langle L_z\rangle$ represents the polarization of the effective spin L.

Taking the general form of V given by Eq. (8), applying an electromagnetic field with angular frequency ω on the L system, considering other relaxation mechanisms represented by $T_{1,2}^{L^{\text{other}}}$, $T_{1,2}^{K^{\text{other}}}$ under the condition $\tau_c \ll \Omega_1^{-1}$, where Ω_1 is the Rabi frequency, and working in the quasiresonant approximation $|\omega - \omega_L| \ll \omega_L$, in the slowly varying envelope approximation, and in the rotating coordinate system, Eq. (25) is written as follows after some lengthy calculations detailed in the Appendix:

(i) *Different L, K systems.*

$$\frac{d\langle L_z\rangle}{dt} = -\frac{3}{4}\frac{1}{T_1^{LL}}(\langle L_z\rangle - \langle L_z\rangle^0) + \frac{3}{4}\frac{1}{T_1^{LK}}(\langle K_z\rangle - \langle K_z\rangle^0) - \frac{1}{T_1^{L^{\text{other}}}}(\langle L_z\rangle - \langle L_z\rangle^0) + \frac{i\Omega_1}{2}(\langle L'_-\rangle - \langle L'_+\rangle), \tag{28}$$

$$\frac{d\langle L'_+\rangle}{dt} = +i\left(\omega_L - \omega + \frac{\langle F_0\rangle}{\hbar}\langle K_z\rangle\right)\langle L'_+\rangle - \frac{1}{T_2^L}\langle L'_+\rangle - i\Omega_1\langle L_z\rangle, \tag{29}$$

$$\frac{d\langle K_z\rangle}{dt}=-\frac{3}{4}\frac{1}{T_1^{KK}}(\langle K_z\rangle-\langle K_z\rangle^0)+\frac{3}{4}\frac{1}{T_1^{LK}}(\langle L_z\rangle-\langle L_z\rangle^0)$$
$$-\frac{1}{T_1^{K^{\text{other}}}}(\langle K_z\rangle-\langle K_z\rangle^0), \tag{30}$$

where $L'_{\pm}=L_{\pm}e^{\pm i\omega t}$. The relaxation rates $1/T_1^{LL}$, $1/T_1^{LK}$, $1/T_2^{L}$, and $1/T_1^{KK}$ are defined in the Appendix. If we apply an electromagnetic field to the *K* system, we obtain similar kinetic equations by replacing *L* by *K* in the above equations.

(ii) *Identical L, K systems*.

$$\frac{d\langle L_z\rangle}{dt}=-\frac{1}{T_1^{L}}(\langle L_z\rangle-\langle L_z\rangle^0)+i\frac{\Omega_1}{2}(\langle L'_-\rangle-\langle L'_+\rangle), \tag{31}$$

$$\frac{d\langle L'_+\rangle}{dt}=i\left[\omega_L-\omega+\left(\frac{\langle F_0\rangle}{\hbar}-2\frac{\langle F_1\rangle}{\hbar}\right)\langle L_z\rangle\right]\langle L'_+\rangle-\frac{1}{T_2^{L}}\langle L'_+\rangle$$
$$-i\Omega_1\langle L'_z\rangle, \tag{32}$$

where the relaxation terms $1/T_1^L$ and $1/T_2^L$ are defined in the Appendix.

The factorization operation shifts the resonance frequency of the transition by $\langle F_0\rangle/\hbar\langle K_z\rangle$ and $(\langle F_0\rangle/\hbar-2\langle F_1\rangle/\hbar)\langle L_z\rangle$ for different and identical *L*, *K* systems, respectively. For identical systems, $\langle F_0\rangle=2\langle F_1\rangle$ when the interaction *V* is only a scalar interaction, which implies that there is no shift in this case. Therefore, for identical *L*, *K* systems in scalar interaction, it is not possible to obtain a bistability phenomenon because there is no renormalization of the resonance frequency, a result already obtained by Heber.[21] Moreover, it is important to notice that even for a very general interaction given by Eq. (8), a lot of terms can be neglected as a consequence of the quasiresonant and the slowly varying envelope approximations (see the Appendix), and only the F_0 and F_1 terms participate in the shift of the resonance.

III. CONDITION FOR INTRINSIC OPTICAL BISTABILITY

A. Steady-state solutions of the kinetic equations

Let us consider successively the two situations where *L*, *K* systems are different or identical. Under steady-state conditions, the time derivative in the kinetic equations (28)–(32) equals zero.

(i) *Different L, K systems*. Equation (30) gives

$$\langle K_z\rangle=\langle K_z\rangle^0-f_L\langle L_z\rangle^0 s_L, \tag{33}$$

where

$$f_L=\frac{3}{4T_1^{LK}\left(\dfrac{3}{4T_1^{KK}}+\dfrac{1}{T_1^{K^{\text{other}}}}\right)} \tag{34}$$

and

$$s_L=\frac{\langle L_z\rangle^0-\langle L_z\rangle}{\langle L_z\rangle^0}. \tag{35}$$

f_L is called the leakage factor and characterizes the efficiency of the polarization transfer from the effective spin *L* ($\langle L_z\rangle$) to the effective spin *K* ($\langle K_z\rangle$), with $0\leqslant f_L\leqslant 1$. When the *V* interaction is the only relaxation mechanism for the *K* system, f_L is maximum and in some cases can be equal to 1. If other relaxation mechanisms coexist with *V*, then f_L is lesser than 1 [see Eq. (34)]. s_L is the saturation factor that can vary between $s=0$ (thermal equilibrium) to $s=1$ (equality of populations). This factor is directly proportional to the intensity of the transition.

Let ω_L^{eff} denote the effective resonant angular frequency of the *L* system,

$$\omega_L^{\text{eff}}=\omega_L+\frac{\langle F_0\rangle}{\hbar}\langle K_z\rangle=\omega_L+\Delta\omega_L \tag{36}$$

where $\Delta\omega_L$ is the renormalization of the resonant frequency ω_L. The maximum value $\Delta\omega_L^{\max}$ of $\Delta\omega_L$ is given by

$$\Delta\omega_L^{\max}=\frac{f_L\langle F_0\rangle\langle L_z\rangle^0}{\hbar}. \tag{37}$$

In this equation $\langle L_z\rangle^0$ is the polarization at thermal equilibrium, which is proportional to the inversion population [Eq. (26)].

In the case of magnetic resonance spectroscopy, $\hbar\omega_L$ is small compare to the thermal energy k_BT. The thermal equilibrium polarization $\langle L_z\rangle^0$ is thus temperature dependent. In the high-temperature approximation and for an effective spin $L=\frac{1}{2}$, $\langle L_z\rangle^0=-\hbar\omega_L/4k_BT$, $\Delta\omega_L^{\max}$ is thus given by

$$\Delta\omega_L^{\max}=-\frac{f_L\langle F_0\rangle\omega_L}{4k_BT}. \tag{38}$$

In the case of infrared and visible spectroscopy, $\hbar\omega_L$ is high compared to the thermal energy k_BT and then $\langle L_z\rangle^0$ is temperature independent. In this spectroscopic range, from low to ambient temperature, only the ground state is populated, that is, $\langle L_z\rangle^0=-\frac{1}{2}$ and $\Delta\omega_L^{\max}$ is thus given by

$$\Delta\omega_L^{\max}=-\frac{f_L\langle F_0\rangle}{2\hbar}. \tag{39}$$

By combining Eqs. (33)–(37), we obtain

$$s_L=\frac{\Omega_1^2T_1^LT_2^L}{1+T_2^{L^2}(\omega_L^{\text{eff}}-\omega)^2+\Omega_1^2T_1^LT_2^L}, \tag{40}$$

$$s_L=-(\omega_L^{\text{eff}}-\omega_L^{\text{eff}\,0})\frac{1}{\Delta\omega_L^{\max}}=\frac{\omega_L^{\text{eff}\,0}-\omega}{\Delta\omega_L^{\max}}-\frac{\omega_L^{\text{eff}}-\omega}{\Delta\omega_L^{\max}}, \tag{41}$$

which correspond to Eqs. (4) and (5) defined in the Introduction and to Fig. 1. The angular frequency $\omega_L^{\text{eff}\,0}$ corresponds to ω_L^{eff} at thermal equilibrium and the longitudinal and transverse relaxation terms T_1^L and T_2^L are written as follows:

$$\frac{1}{T_1^L}=-\frac{3}{4}\left(\frac{1}{T_1^{LK}}f_L-\frac{1}{T_1^{LL}}\right)+\frac{1}{T_1^{L^{\text{other}}}}, \tag{42}$$

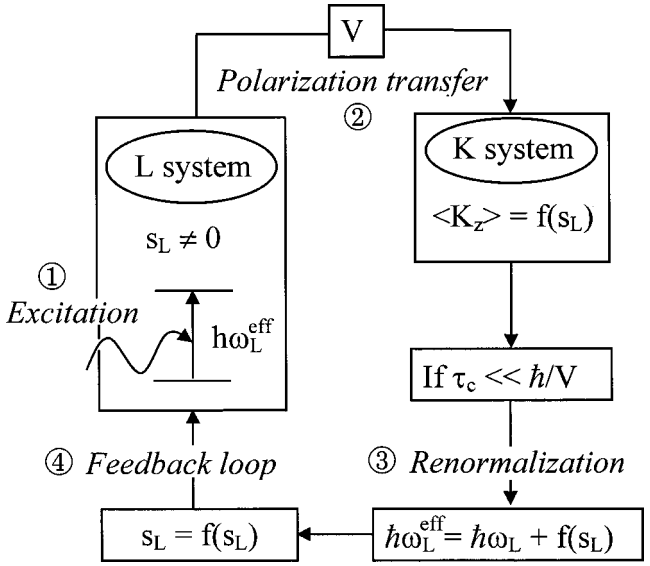

FIG. 2. Four-step mechanism of bistability. The system under study is composed of two weakly interacting subsystems L and K. The first step represents the nonlinear process: excitation of the L system with a resonant electromagnetic field. The second step represents the polarization transfer between L and K, and the time average $\langle K_z \rangle$ becomes a function of the saturation factor s_L [Eq. (33)]. In the third step, ω_L^{eff} is renormalized and becomes a function of s_L [Eq. (36)] under the condition $\tau_c \ll \hbar/V$. The fourth step represents the feedback loop where the saturation factor becomes a function of itself $s_L = f(s_L)$ [Eqs. (40) and (41)].

$$\frac{1}{T_2^L} = \frac{1}{T_2^{L\,\text{int}}} + \frac{1}{T_2^{L\,\text{other}}}. \tag{43}$$

(ii) *Identical L, K systems*. By the same procedure, Eqs. (31) and (32) in steady-state conditions give Eqs. (40) and (41) with ω_L^{eff} and $\Delta\omega_L^{\max}$

$$\omega_L^{\text{eff}} = \omega_L + \left(\frac{\langle F_0 \rangle}{\hbar} - 2\frac{\langle F_1 \rangle}{\hbar} \right) \langle L_z \rangle, \tag{44}$$

$$\Delta\omega_L^{\max} = \left(\frac{\langle F_0 \rangle}{\hbar} - 2\frac{\langle F_1 \rangle}{\hbar} \right) \langle L_z \rangle^0 \tag{45}$$

and

$$\frac{1}{T_1^L} = -\frac{3}{4}\left(\frac{1}{T_1^{LK}} - \frac{1}{T_1^{LL}} \right) + \frac{1}{T_1^{L\,\text{other}}}, \tag{46}$$

$$\frac{1}{T_2^L} = \frac{1}{T_2^{L\,\text{int}}} + \frac{1}{T_2^{L\,\text{other}}}. \tag{47}$$

It is interesting to note that there is no leakage factor when L and K are identical. Moreover, Eqs. (44) and (45) clearly show that there is no shift of the frequency, and thus no possibility of bistability for a scalar interaction between L and K, as $\langle F_0 \rangle = 2\langle F_1 \rangle$ in this case.

All the previous calculations can be summarized by a four-step mechanism (Fig. 2). The system under study is composed of two weakly interacting subsystems L and K. The first step is the excitation of the L system with a resonant electromagnetic field, which is, even for a very simple two-level system, a nonlinear process. In the second step, a polarization transfer occurs between L and K through the interaction V, and the polarization $\langle K_z \rangle$ of the K system becomes a function of the saturation factor s_L [Eq. (33)]. In the third step, if the interaction fluctuates such as the condition $\tau_c \ll \hbar/V$ is fulfilled, the effective resonant angular frequency of the L system ω_L^{eff} is renormalized, which means that ω_L^{eff} becomes a function of s_L [Eq. (36)]. In the fourth step, as ω_L^{eff} changes continuously during the excitation, the saturation factor becomes a function of itself $s_L = f(s_L)$, which corresponds to the feedback loop [Eqs. (40) and (41)]. This self-consistent equation is a third-degree equation that can exhibit three solutions—a signature of bistablity.

B. Condition for the occurrence of bistability

If we except the particular case of two identical L, K systems in scalar interaction, the L system becomes bistable when the straight line of Eq. (41) exhibits three crossing points with the curve of Eq. (40) as shown in Fig. 1(a). This situation occurs when the slope of Eq. (41) is smaller than the tangent at the inflection point of the curve of Eq. (40). On the left side of Eq. (40), this condition gives

$$|\Delta\omega_L^{\max}| > \frac{8}{3\sqrt{3}T_2^L} \frac{1}{s_L^r \sqrt{1 - s_L^r}} \tag{48}$$

with $s_L^r = \Omega_1^2 T_1^L T_2^L / (1 + \Omega_1^2 T_1^L T_2^L)$ being the saturation factor at the resonance [$\omega = \omega_L^{\text{eff}}$ in Eq. (40)]. This condition can be generalized by taking the value of s_L^r that minimizes the right side of Eq. (48), that is, $s_L^r = \frac{2}{3}$, which gives for the bistability condition

$$|\Delta\omega_L^{\max}| > \frac{4}{T_2^L}, \tag{49}$$

where $|\Delta\omega_L^{\max}|$ and T_2^L are given in $\text{rad}\,\text{s}^{-1}$ and seconds respectively.

Finally, there should exist at least one value of the control parameters that can give three solutions for Eqs. (40) and (41) when condition (49) is fulfilled. Three control parameters can be varied experimentally: (i) the incident power of the electromagnetic field, proportional to the square of the Rabi frequency Ω_1^2, (ii) the angular frequency ω of the incident field, and (iii) the external temperature. Equation (49) can be rewritten by considering the homogeneous linewidth Γ_h of the transition given by $\Gamma_h = 1/\pi T_2^L$:

$$|\Delta\omega_L^{\max}| > 2\Gamma_h, \tag{50}$$

where $|\Delta\omega_L^{\max}|$ and Γ_h are given in cm^{-1}.

As a conclusion, in order to obtain a bistable "shark fin" shape as shown in Fig. 1(b), the maximum shift of the frequency induced by the fluctuating interaction must be larger than twice the homogeneous linewidth of the transition.

C. Discussion of the parameters controlling IOB

All the equations obtained in the previous part are controlled by different parameters, which can be separated into two classes: those related to the structure and properties of the solid (internal parameters) and those that can be controlled experimentally (external parameters). The internal parameters are the longitudinal and transverse relaxation times, T_1^L and T_2^L, the leakage factor f_L that depends on all the possible relaxation mechanisms, and the interaction V between the two L and K subsystems. The control parameters are the frequency of the incident field ω and the power P of the incident field linked to the Rabi frequency by the following equation:

$$P = \frac{mc\epsilon_0}{q^2}\frac{\hbar\omega_L}{F_{ab}}\Omega_1^2, \tag{51}$$

where F_{ab} is the oscillator strength of the transition, m and q are the electron mass and charge, respectively, and ϵ_0 is the permittivity of the vacuum. The temperature is also a ''hidden'' control parameter, as it may influence the relaxation terms as well as the maximum shift of the frequency $\Delta\omega_L^{\max}$ through the leakage factor, and in the case of magnetic resonance spectroscopies ($\hbar\omega_L \ll k_B T$) through the thermal equilibrium population [see Eq. (38)].

When the system is under bistable conditions, all the control parameters ω, P, and T can produce a bistable response of the transition. In the following we will only focus on the frequency ω and the power P of the external field. Indeed, the influence of the temperature on the relaxation terms can be very different from one system to another and thus cannot be discussed in a general way. Consequently we consider the two possible cases of bistable response: a hysteresis induced by upward and downward sweeps of the frequency [Fig. 3(a)] and a hysteresis induced by a variation of the incident power [Fig. 3(b)]. In the first case, the position of the line of Eq. (41) and the amplitude of the bell-shaped curve of Eq. (40) are kept constant. The variation of the frequency ω corresponds to a horizontal shift of Eq. (40). In the case of a hysteresis induced by a variation of the incident power, the positions of the straight line and of the bell-shaped curve are fixed. Increasing the power P of the incident field leads to a broadening and an increase of the bell-shaped curve [Fig. 3(b)].

The effects of the internal parameters on the bistable response are gathered in Figs. 4–6, which represent the effects of the leakage factor f_L, the longitudinal relaxation term T_1^L, and the transverse relaxation term T_2^L, respectively. Each simulation in Figs. 4–6 is obtained by a numerical resolution of the coupled equations (40) and (41). Both the frequency-induced hysteresis [Figs. 4(a), 5(a), and 6(a)] and the power-induced hystereses [Figs. 4(b), 5(b), and 6(b)] are shown. All the simulations are performed with dimensionless parameters.

The leakage factor f_L influences the bistability as shown in Figs. 4(a) and 4(b). The figures are calculated for $f_L=0$, 0.1, 0.2, 0.4, 0.6, and 1, which correspond to $|\Delta\omega_L^{\max}|T_2^L = 0$, 1, 2, 4, 6, and 10, respectively. T_1^L and T_2^L are fixed in the simulation. The transitions of Fig. 4(a) are calculated with a fixed value of the incident power, indicated by an arrow in Fig. 4(b). The hysteresis curves of Fig. 4(b) are calculated with a fixed value of the incident frequency, indicated by an arrow in Fig. 4(a). The leakage factor influences $\Delta\omega_L^{\max}$ [Eq. (37)] and thus the shape of the bent transition as shown in Fig. 4(a). When f_L increases, the shape of the line becomes more and more asymmetrical until a critical point corresponding to $f_L=0.4$ (and thus to $|\Delta\omega_L^{\max}|T_2^L=4$), where the system becomes bistable. As already shown in Sec. II B, the boundary between the monostable and bistable situations corresponds to $|\Delta\omega_L^{\max}|T_2^L=4$. For $|\Delta\omega_L^{\max}|T_2^L \geqslant 4$, the response of the system becomes dependent on the sweep direction of the frequency as well as on the sweep direction of the incident power as shown in Fig. 4(b). For $f_L<0.4$, the intensity remains independent of the power sweep direction. When f_L increases in the bistable regime [Fig. 4(b)], the hysteresis loop is shifted towards lower power and appears for a lower value of the intensity. All these simulations reflect the effects of the maximum frequency shift $\Delta\omega_L^{\max}$ through the leakage factor on the bistable response of the system.

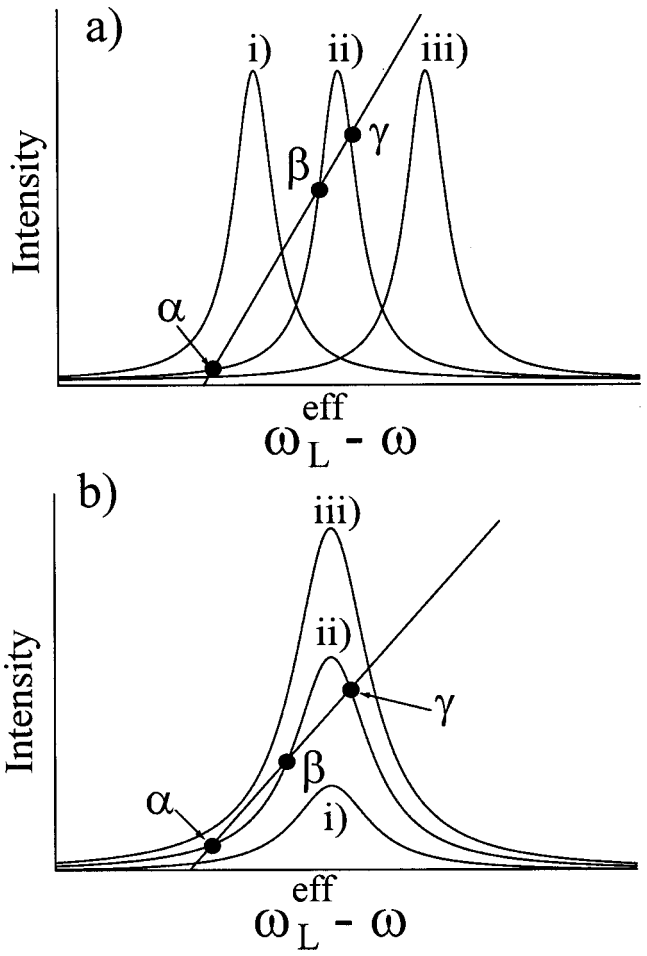

FIG. 3. Origin of the frequency-induced hysteresis (a) and the power induced-hysteresis (b). Cases (i)–(iii) correspond to three different values of the frequency or of the power of the incident electromagnetic field. Case (ii) corresponds to a bistable situation with three crossing points (α, β, γ).

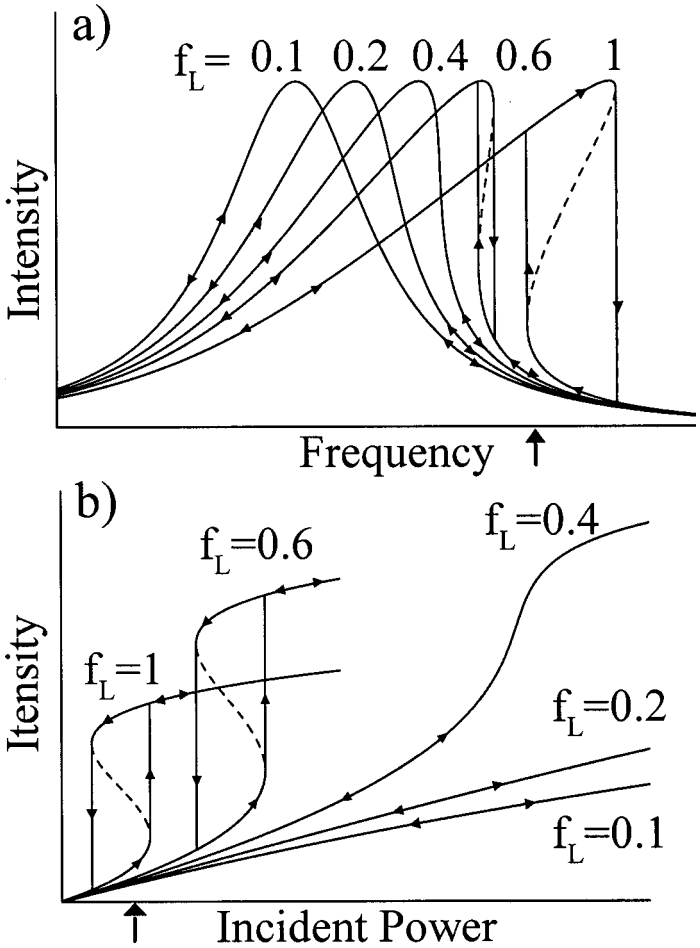

FIG. 4. Effect of the leakage factor f_L on optical bistability. The simulations are performed with dimensionless parameters. T_1^L, T_2^L are fixed and $\Delta\omega_L^{\max}$ is taken as negative. (a) Intensity versus frequency, the power is set at the value indicated by an arrow in (b). (b) Intensity versus incident power, the frequency is set at the value indicated by an arrow in (a). $f_L=0.1$, 0.2, 0.4, 0.6, and 1 correspond to $|\Delta\omega_L^{\max}|T_2^L$=1, 2, 4, 6, and 10, respectively. The critical point between the monostable and bistable situation is found for $|\Delta\omega_L^{\max}|T_2^L$=4.

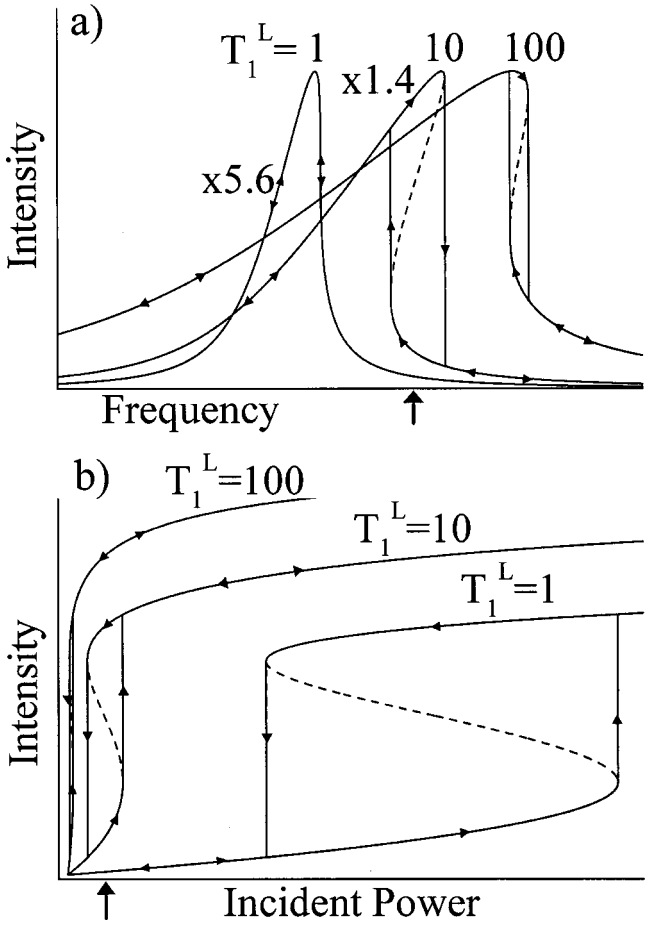

FIG. 5. Effect of the longitudinal relaxation term T_1^L on optical bistability. The simulations are performed with dimensionless parameters. $\Delta\omega_L^{\max}<0$ and T_2^L are fixed with $|\Delta\omega_L^{\max}|T_2=10$. (a) Intensity versus frequency, the power is set at the value indicated by an arrow in (b). (b) Intensity versus incident power, the frequency is set at the value indicated by an arrow in (a).

Figures 5(a) and 5(b) gather the effects of the longitudinal relaxation term T_1^L, which is directly linked to the lifetime of the excited state of the transition. All the simulations are performed with a fixed value of $\Delta\omega_L^{\max}<0$ and T_2^L corresponding to $|\Delta\omega_L^{\max}|T_2^L=10$. The transitions of Fig. 5(a) are obtained with a fixed value of the incident power [indicated by an arrow in Fig. 5(b)], and the curves of Fig. 5(b) are obtained with a fixed value of the incident frequency [indicated by an arrow in Fig. 5(a)]. When T_1^L increases, the intensity of the transition increases [see the multiplication factors in Fig. 5(a)]. This can also be seen in Fig. 5(b) for high T_1^L, where the intensity reaches its limit value for lower power of the incident field. For high T_1^L, the transition is more easily saturable. The most important influence of T_1^L is shown in Fig. 5(b). By increasing T_1^L, the hysteresis loop shifts towards lower power as the transition can be saturated more easily, and the width of the hysteresis loop drastically decreases. T_1^L has thus a strong influence on the bistable properties, and a long T_1^L is preferable as the phenomenon can be obtained for low power of the incident field.

The effects of the transverse relaxation terms T_2^L are gathered in Figs. 6(a) and 6(b). All the simulations are obtained with fixed values of T_1^L and $\Delta\omega_L^{\max}<0$. The values $T_2^L=1$, 4, 10, and 50 correspond to $|\Delta\omega_L^{\max}|T_2^L$=1, 4, 10, and 50 in our simulations. The effect of T_2^L is different from that of T_1^L. When T_2^L increases, the homogeneous linewidth $\Gamma_h=1/\pi T_2^L$ of the transition decreases. Moreover, in the bistable regime, increasing T_2^L does not induce an important shift in the position of the hysteresis loop as previously seen for T_1^L, but the width of the loop drastically increases revealing a strongly bent transition as shown in Fig. 6(a).

From the previous simulations we can conclude that the system L will exhibit a bistability if the following conditions are fulfilled: (i) The homogeneous transition linewidth should be very small implying a long transverse relaxation time T_2^L. (ii) The longitudinal relaxation T_1^L should be sufficiently long to obtain a moderate saturability of the transition at rather low incident power. (iii) $|\Delta\omega_L^{\max}|$ should be high

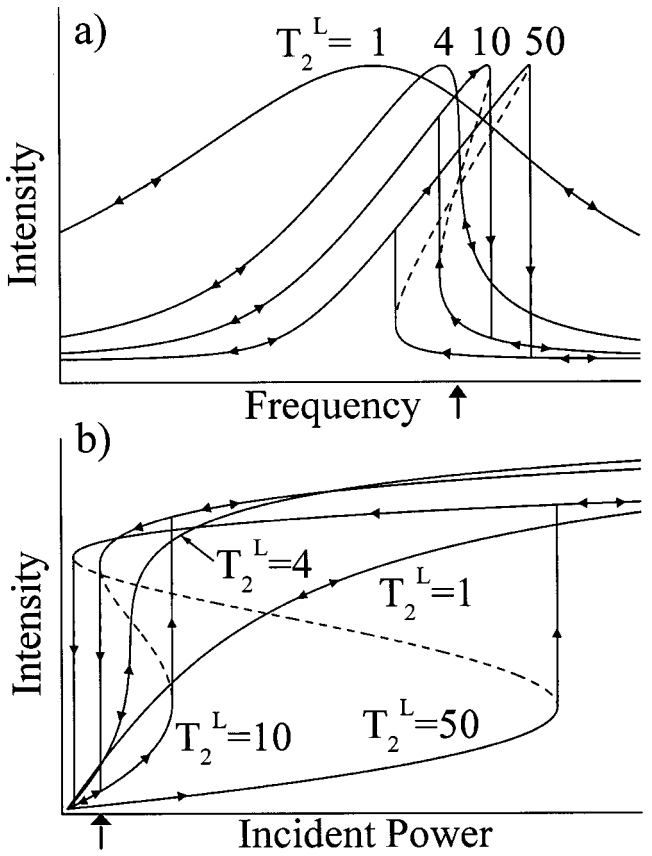

FIG. 6. Effect of the transverse relaxation term T_2^L on optical bistability. The simulations are performed with dimensionless parameters. T_1^L and $\Delta\omega_L^{\max}<0$ are fixed. (a) Intensity versus frequency, the power is set at the value indicated by an arrow in (b). (b) Intensity versus incident power, the frequency is set at the value indicated by an arrow in (a). $T_2^L=1$, 4, 10, and 50 correspond to $|\Delta\omega_L^{\max}|T_2^L=1$, 4, 10, and 50, respectively. The critical point between the monostable and bistable situation is found for $|\Delta\omega_L^{\max}|T_2^L=4$.

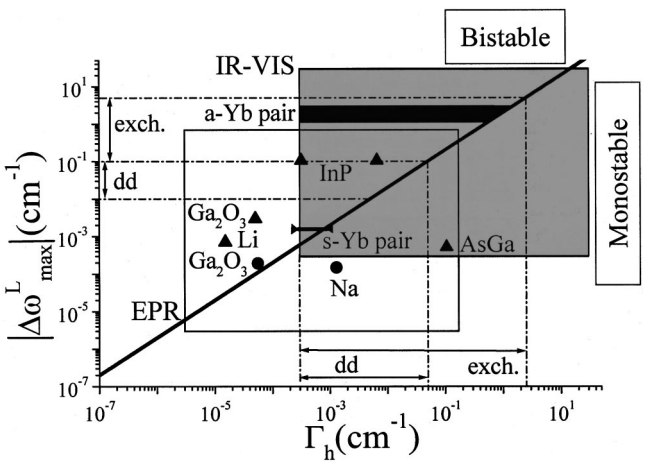

FIG. 7. Theoretical phase diagram presenting the condition for an intrinsic spectroscopic bistability representing the maximum shift $|\Delta\omega_L^{\max}|$ (cm^{-1}) of the transition versus the homogenous linewidth $\Gamma_h=1/\pi T_2^L$ (cm^{-1}). The circles and triangles are experimental data obtained in the microwave range. They correspond to experiments at ambient and liquid-helium temperature, respectively. dd corresponds to magnetic dipole-dipole interactions and to the Lorentz local-field correction, exch. corresponds to electric multipole interactions, electronic exchange interactions, and virtual phonon exchange interactions. *a* pair and *s* pair means asymmetric and symmetric pairs of ytterbium ions in $CsCdBr_3$.

enough implying a strong interaction V between the two subsystems and a high value of the leakage factor f_L. To obtain a strong f_L, the relaxation rate $1/T_1^{K^{\text{other}}}$ has to be very small compared to $1/T_1^{KK}$ [see Eq. (34)], which means that the relaxation terms of the K system induced by the interaction V should be predominant in order to maximize the value of f_L. All the other relaxation terms of the K system contribute to a decrease of the efficiency of the polarization transfer between the two subsystems. It is important to notice that V should be strong enough to give high value of $|\Delta\omega_L^{\max}|$, but not too strong. Indeed, the previous treatment is based on the two conditions $|V|\ll|H_K|$, $|H_L|$, $|H_M|$ and $\tau_c\ll\hbar/V$, which implies that we can perform a perturbation treatment of the spin Hamiltonian and that τ_c is fast enough to average the V interaction. The condition $\tau_c\ll\hbar/V$ gives the higher limit of V. If we assume that a lower limit of τ_c is 10^{-13} s, which corresponds to a typical correlation time for the motion of conduction electrons in semiconductors, and if we assume that the condition $\tau_c\ll\hbar/V$ gives a ratio $\hbar/V$ at least one order of magnitude higher than τ_c, then we get $V\leqslant 30\ \text{cm}^{-1}$.

From the criterion $|\Delta\omega_L^{\max}|>2\Gamma_h$ [Eq. (50)], it is possible to draw a phase diagram by plotting $|\Delta\omega_L^{\max}|$ versus Γ_h (Fig. 7). The straight line corresponds to $|\Delta\omega_L^{\max}|=2\Gamma_h$ and defines the boundary between the lower monostable domain and the upper bistable domain. Two spectroscopic ranges are considered in Fig. 7: the microwave range corresponding mainly to electron paramagnetic resonance (EPR) and represented by an open rectangle in Fig. 7 and the infrared and visible ranges, which correspond to classical absorption and fluorescence spectroscopies represented by a gray rectangle.

For both cases, the upper and lower limits that define the different domains are not definitive and are only given for indication. For the EPR range, $|\Delta\omega_L^{\max}|$ varies from $\approx 3.3\times10^{-6}$ cm^{-1} up to ≈ 0.67 cm^{-1} ($\approx$0.1 MHz to $\approx$20 GHz) and Γ_h from $\approx 3.3\times10^{-6}$ cm^{-1} up to ≈ 0.17 cm^{-1} ($\approx$0.1 MHz to $\approx$5 GHz). The lower and higher limits of $|\Delta\omega_L^{\max}|$ and Γ_h can be found in organic compounds and in inorganic semiconductors, respectively.[29,30] In order to predict whether a given material can exhibit a bistable EPR response, we report in Fig. 7 some literature data for several conducting materials. The positions of the EPR points in such diagram have already been discussed in Ref. 31. These values correspond to Na,[32] Li,[33] β-Ga_2O_3,[3] and InP,[34] and were obtained from EPR measurements performed on conduction electrons. The measurements were performed at the *X*-band at a magnetic field B_0 of the order of 0.35 T. The circles were obtained at 300 K and the triangles at 4 K. In all cases, the conduction electrons are connected to N nuclear spins by a scalar hyperfine interaction A of the Fermi contact type and $\Delta\omega_L^{\max}$ is thus written as $|\Delta\omega_L^{\max}|=f_L NAg\beta B_0/4k_B T\hbar$, where g is the g factor associated with the conduction electron and

β is the Bohr magneton. This phase diagram predicts that only β-Ga_2O_3 is bistable at ambient temperature. However, InP and metallic lithium particles should give a bistable EPR response at low temperature. These predicted bistable EPR spectra have been observed in β-Ga_2O_3,[3] InP,[4] and in metallic lithium.[5] This phase diagram demonstrates, therefore, its powerful predictability in the microwave range. We will not discuss any further the microwave bistability in this section as all these results have already been published elsewhere. We will come back to the case of β-Ga_2O_3 in Sec. IV A to demonstrate how such a case of bistability is totally justified and explained in the framework of the present approach.

Let us now focus on the infrared or visible range, which is the spectroscopic domain of interest in this work. For this spectroscopic range $|\Delta\omega_L^{\max}|$ and Γ_h vary roughly from $\approx 3\times10^{-4}$ cm^{-1} to $\approx$30 cm^{-1} (10 MHz–1000 GHz). The lower values of $|\Delta\omega_L^{\max}|$ correspond to typical interactions encountered between two rare-earth ions,[35] and the higher values correspond to the interaction between two transitions ions (see the case of chromium ion pairs in ruby for example).[36] The higher limit of $|\Delta\omega_L^{\max}| \leqslant 30$ cm^{-1} is fixed by the condition $\tau_c \ll \hbar/V$ as discussed previously in this section. The lower limit of Γ_h, which gives also the lower limit of the measurable $|\Delta\omega_L^{\max}|$, can be obtained for rare-earth ions with coherent transient and hole-burning spectroscopy.[37] High-resolution Fourier transform spectroscopy can measure an interaction of a few 10^{-3} cm^{-1} in the infrared and visible ranges. In the case of Ref. 38, for example, Chukalina *et al.* report the first observation of a resolved hyperfine structure of 10^{-2} cm^{-1} and 7×10^{-3} cm^{-1} in the $^4I_{15/2}\rightarrow{}^4I_{13/2}$ infrared transition of $LiYF_4$:Er. In the phase diagram of Fig. 7, we divide the infrared and the visible range into two domains depending on the nature of the V interaction. The first domain denoted dd in Fig. 7 and ranging from 10^{-2} to 10^{-1} cm^{-1} corresponds to magnetic dipole-dipole interactions and to the Lorentz local-field correction based on an electric dipole-dipole interaction. The second domain denoted exch. and ranging from 10^{-1} to 10 cm^{-1} corresponds to electric multipole interactions, electronic exchange, and virtual phonon exchange interactions.[35] For example, Guillot-Noël *et al.* have shown that satellites in electron paramagnetic resonance and in high-resolution fluorescence spectra of neodymium in $LiYF_4$ and YVO_4 matrices are due to Nd^{3+}-Nd^{3+} pairs with the magnetic dipole-dipole interaction varying from 10^{-2} to 2×10^{-2} cm^{-1} and the ground-state exchange interaction J varying from 0.8 to 4.9 cm^{-1}.[39] Basiev *et al.* demonstrated that a strong quadrupole-quadrupole interaction of 5 cm^{-1} between two neodymium ions is responsible for an observed fine splitting of the excited Kramers levels in Nd:CaF_2 compounds.[40] Exchange interaction can reach higher values in the case of transition ions. In ruby, for example, exchange interactions in chromium ion pairs can reach 240 cm^{-1}.[36] In the case of the Lorentz local-field correction based on a ground-state dipole-dipole interaction,

$$|\Delta\omega_L^{\max}| = \frac{N}{6\varepsilon_0}\frac{q^2}{m}\frac{F_{ab}}{\omega_L},$$

where N is the number of absorbing ions per unit volume.[13,17] This interaction gives values of $\Delta\omega_L^{\max}$ that are usually in the range $\approx5\times10^{-2}$ to $\approx10^{-1}$ cm^{-1}. For example, in $Cs_3Y_2Br_9$:10% Yb, $|\Delta\omega_L^{\max}|\approx5\times10^{-2}$ cm^{-1} with $N=4\times10^{20}$ atoms/cm^3, $F_{ab}=2\times10^{-6}$, and $\hbar\omega_L = 10\,120$ cm^{-1}.[41] In YVO_4:0.58% Nd, where neodymium ions exhibit high oscillator strengths, $|\Delta\omega_L^{\max}|\approx10^{-1}$ cm^{-1} with $N=7.25\times10^{19}$ atoms/cm^3, $F_{ab}=50\times10^{-6}$, and $\hbar\omega_L = 20\,000$ cm^{-1}.[42]

A bistable response due to a fluctuating magnetic dipole-dipole-type interaction or due to the Lorentz local-field correction ($\tau_c \ll \hbar/V$ and the dd domain ranging from 10^{-2} to 10^{-1} cm^{-1}) implies a homogeneous linewidth of the transition lower than 0.05 cm^{-1} (Fig. 7). This linewidth is difficult to obtain at ambient temperature, where the homogeneous broadening is typically of 1 to 10 cm^{-1} for rare-earth ions (see, for example, Ref. 43) and can be broader for transition ions. The dominant contribution to the homogeneous linewidth at ambient temperature is due to the interaction with the lattice through one-phonon, multiphonon, Raman two-phonon scattering processes. However, at a very low temperature (liquid-helium temperature), a homogeneous linewidth of 0.05 cm^{-1} can be obtained for some rare-earth transitions,[37,38] and then a bistability may exist. The phase diagram of Fig. 7 shows that a bistability phenomenon based only on the Lorentz local-field correction is probably difficult to obtain at ambient temperature and becomes possible at very low temperature. However, in the cases of electric multipole interaction, electronic exchange interaction, and virtual phonon exchange interaction, which can reach a few cm^{-1}, a bistable response can exist at ambient temperature. For example, a maximum $\Delta\omega_L^{\max}$ shift of 2 cm^{-1} requires at maximum a homogeneous linewidth of 1 cm^{-1}.

IV. APPLICATION OF THE EFFECTIVE SPIN-HAMILTONIAN APPROACH TO REAL SYSTEMS

A. In the microwave range: Bistability of the magnetic resonance of electrons in solids

In this part we apply the model to a bistable situation in which the L system is a real electron spin. As mentioned in the Introduction, bistable electron magnetic resonance has been observed in several types of conductors (metal and semiconductors).[3–5] Gallium oxide β-Ga_2O_3 is a well-documented example of intrinsic EPR bistability.[3] This compound is normally an isolator with a forbidden energy gap of 4.8 eV. However, it is generally an n-type semiconductor due to oxygen vacancies compensated by two electrons. The unpaired electron spins exhibit hyperfine interactions (of the Fermi contact type) with the ^{69}Ga and the ^{71}Ga nuclei, which posses a nuclear spin equal to $\frac{3}{2}$ and a natural abundance of 60.1% and 39.9%, respectively. Let us call L the electron-spin system and K the system composed of N equivalent Ga nuclei. Each system is represented by an effective spin equal to $\frac{1}{2}$. For the electron, it is a real spin but in the case of the Ga nuclei, it is an effective spin. The spin Hamiltonian of a unpaired conduction electron L interacting with N equivalent nuclear spins K by a scalar hyperfine interaction A under an external constant field B_0 is written as

$$H = H_L + H_K + H_M + V \tag{52}$$

with $H_L = g\beta B_0 L_z$, $H_K = -g_n \beta_n B_0 K_z$, and

$$V = AL_z\left(\sum_{p=1}^{N} K_{z,p}\right) + \frac{A}{2}\left[L_+\left(\sum_{p=1}^{N} K_{-,p}\right) + L_-\left(\sum_{p=1}^{N} K_{+,p}\right)\right], \tag{53}$$

where β and β_n are the electron Bohr magneton and nuclear Bohr magneton, respectively, g and g_n are the g factors of the electron and the nucleus, respectively.

Since the effective spin-Hamiltonian approach of bistability is based on the different time scales of the system under study, it is first necessary to identify the different characteristic times controlling the spin dynamics. First of all, if we look carefully at the EPR spectrum of conduction electrons in β-Ga_2O_3 [see Fig. 8(a)], it is composed of a narrow single line with a average width of 0.05 mT at room temperature and low microwave power. The expected hyperfine structure coming from the interaction between the two subsystems L and K is not visible in the spectra showing that we are under the condition $\tau_c \ll \hbar/A$. Indeed, as previously shown in Sec. II B, the hyperfine interaction V is not observed in the spectrum and the transition is expected to be narrow under this condition. The correlation time τ_c of the hyperfine interaction is imposed by the electronic motion in the conduction band. τ_c is typically of the order of $\tau_c = 10^{-13}$ s in β-Ga_2O_3. As the gallium hyperfine interaction is $A \sim 7800$ MHz,[3] giving $\hbar/A \sim 10^{-8}$ s, then the condition $\tau_c \ll \hbar/A$ is fulfilled. Therefore, the previous approach is totally justified in this case.

The relaxation times T_1^{LL}, T_1^{KK}, $T_2^{L\,\mathrm{int}}$, $T_2^{K\,\mathrm{int}}$ due to the hyperfine interaction are of the order of 10^{-1}–1 s.[3] Other relaxation mechanisms have to be taken into account. For the L system, we have to consider the electron-spin–lattice relaxation time $T_1^{L\,\mathrm{other}}$ and the electron-spin–spin relaxation time $T_2^{L\,\mathrm{other}}$, both are of the order of 10^{-7} s.[3] For the K system, we have to consider other relaxation terms such as the nuclear-spin–lattice relaxation time and in the case of nuclei with nuclear spin higher than $\frac{1}{2}$, the quadrupolar relaxation time. These terms $T_{1,2}^{K\,\mathrm{other}}$ are of the order of a few seconds.[3]

Under the condition $\tau_c \ll \hbar/A$, and using the same approximations as for Eqs. (28)–(30), these kinetic equations for the spin system are written as

$$\frac{d\langle L_z\rangle}{dt} = -\frac{3}{4}\frac{1}{T_1^{LL}}[(\langle L_z\rangle - \langle L_z\rangle^0) - (\langle K_z\rangle - \langle K_z\rangle^0)] - \frac{1}{T_1^{L\,\mathrm{other}}}(\langle L_z\rangle - \langle L_z\rangle^0) + \frac{i\Omega_1}{2}(\langle L'_-\rangle - \langle L'_+\rangle), \tag{54}$$

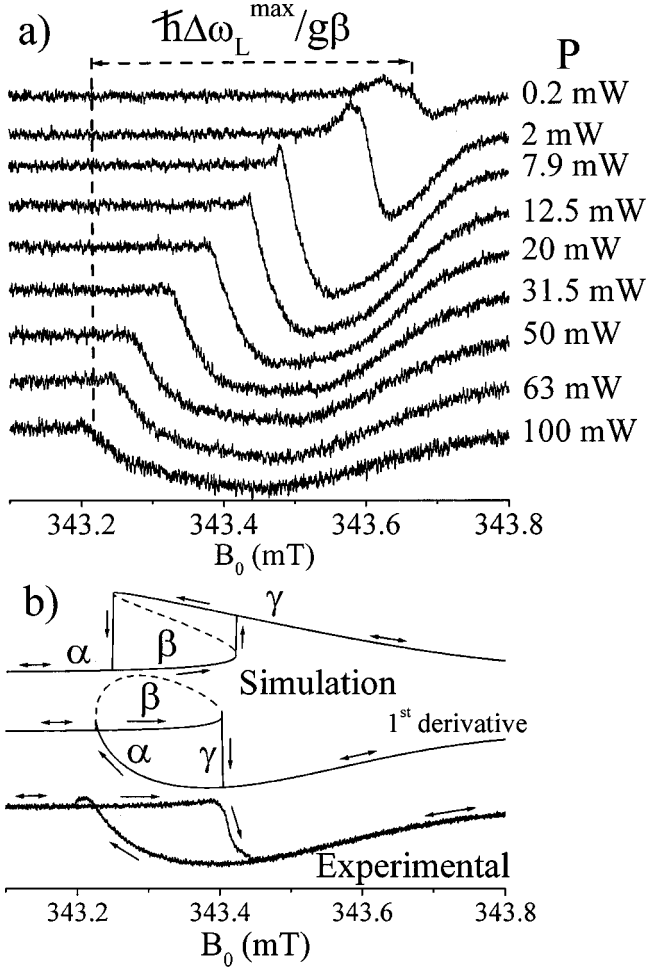

FIG. 8. (a) Experimental proof of the renormalization of the resonance frequency in EPR spectroscopy. The spectra are performed on β-Ga_2O_3 single crystal and recorded as an absorption derivative under decreasing variations of the external magnetic field B_0 and at $T = 150$ K. The microwave power increases from the top to the bottom of the figure. Experimental conditions: microwave frequency, 9.432 76 GHz; sweeping time, 0.012 mT/s; time constant, 41 ms; modulation amplitude, 0.01 mT; modulation frequency, 100 kHz. (b) Selected experimental and simulated bistable EPR spectra at $T = 150$ K, $P = 63$ mW. The simulations before and after derivation are shown. The parameters of the simulation are $P = 63$ mW, $\hbar\omega_L = 0.31\ \mathrm{cm}^{-1}$, $T_1^L = 1.9\times10^{-7}$ s; $T_2^L = 1.45\times10^{-7}$ s corresponding to $\Gamma_h = 7.3\times10^{-5}\ \mathrm{cm}^{-1}$, $\Delta\omega_L^{\max} = -4.3\times10^{-4}\ \mathrm{cm}^{-1}$, $|\Delta\omega_L^{\max}|T_2^L = 12$.

$$\frac{d\langle L'_+\rangle}{dt} = i\left(\omega_L - \omega + \frac{NA}{\hbar}\langle K_z\rangle\right)\langle L'_+\rangle - \frac{1}{T_2^L}\langle L'_+\rangle - i\Omega_1\langle L_z\rangle, \tag{55}$$

$$\frac{d\langle K_z\rangle}{dt} = -\frac{3}{4}\frac{1}{T_1^{KK}}[(\langle K_z\rangle - \langle K_z\rangle^0) - (\langle L_z\rangle - \langle L_z\rangle^0)] - \frac{1}{T_1^{K\,\mathrm{other}}}(\langle K_z\rangle - \langle K_z\rangle^0) \tag{56}$$

with $\Omega_1 = g\beta B_1$ being the Rabi frequency. As $1/T_{1.2}^{LL} \ll 1/T_{1.2}^{L\,\mathrm{other}}$, Eqs. (54) and (55) become

$$\frac{d\langle L_z\rangle}{dt} = -\frac{1}{T_1^{L\,\text{other}}}(\langle L_z\rangle - \langle L_z\rangle^0) + \frac{i\Omega_1}{2}(\langle L'_-\rangle - \langle L'_+\rangle), \tag{57}$$

$$\frac{d\langle L'_+\rangle}{dt} = i\left(\omega_L - \omega + \frac{NA}{\hbar}\langle K_z\rangle\right)\langle L'_+\rangle - \frac{1}{T_2^{L\,\text{other}}}\langle L'_+\rangle - i\Omega_1\langle L_z\rangle. \tag{58}$$

Under steady-state conditions, the saturation factor [Eq. (35)] is given by

$$s_L = \frac{\Omega_1^2 T_1^{L\,\text{other}} T_2^{L\,\text{other}}}{1 + T_2^{L\,\text{other}^2}(\omega_L^{\text{eff}} - \omega)^2 + \Omega_1^2 T_1^{L\,\text{other}} T_1^{L\,\text{other}}}, \tag{59}$$

$$s_L = -(\omega_L^{\text{eff}} - \omega_L^{\text{eff}^0})\frac{1}{\Delta\omega_L^{\max}} \tag{60}$$

with

$$\omega_L^{\text{eff}} = \omega_L + \frac{NA}{\hbar}\langle K_z\rangle, \tag{61}$$

$$\Delta\omega_L^{\max} = \frac{f_L NA\langle L_z\rangle^0}{\hbar} \sim -\frac{f_L NA g\beta B_0}{4k_B T\hbar} \tag{62}$$

in the high-temperature limit, and with the leakage factor f_L given by

$$f_L = \frac{3}{4T_1^{KK}\left(\frac{3}{4T_1^{KK}} + \frac{1}{T_1^{K\,\text{other}}}\right)}. \tag{63}$$

The factorization operation leads to a renormalization of the resonance frequency of $(NA/\hbar)\langle K_z\rangle$. It means that the nuclear-spin polarization $\langle K_z\rangle$ produces a nuclear field $(NA/g\beta)\langle K_z\rangle$, which adds to the external field B_0. The nuclear-spin polarization and thus the shift of the electronic transition can be considerably enhanced by dynamic nuclear polarization by saturating the EPR signal of conduction electrons. This was predicted in metals by Overhauser[7] and analyzed in detail by Solomon.[25] It is worth noticing that the nuclear field produces a feedback on the electron resonance, which is in turn modified. The resulting modification of the resonance (modification of s_L) implies another modification of the nuclear field via Eq. (56), and so on. The nuclear field becomes a function of itself as well as the saturation factor. The Overhauser effect is thus at the origin of the feedback loop.

Figure 8(a) presents a convincing evidence of the validity of the factorization operation through the observed continuous shift of the resonance frequency. The EPR spectra gathered in Fig. 8(a) have been recorded at 150 K with a decreasing variation of the external magnetic field B_0 and for different values of the incident microwave power P. Upon increasing P, the EPR line distorts and shifts to a low magnetic field as a result of the increase of the nuclear field $(NA/g\beta)\langle K_z\rangle$ originating from the dynamic nuclear polarization. The phase diagram in Fig. 7 predicts a bistable behavior (hysteresis) of the EPR transition in β-Ga_2O_3, which can appear for an upward and downward sweep of the external magnetic field B_0 as well as under increasing and decreasing variations of P.[3] This bistable phenomenon is shown in Fig. 8(b) which gathers experimental and simulated EPR spectra for the two sweep directions of the external magnetic field. This figure presents the simulated spectrum before and after derivation. The parameters of the simulation are $P = 63$ mW, $\hbar\omega_L = 0.31\ \text{cm}^{-1}$, $T_1^L = 1.9\times10^{-7}$ s; $T_2^L = 1.45\times10^{-7}$ s corresponding to $\Gamma_h = 7.3\times10^{-5}\ \text{cm}^{-1}$, $\Delta\omega_L^{\max} = -4.3\times10^{-4}\ \text{cm}^{-1}$, $|\Delta\omega_L^{\max}|T_2^L = 12$. All these parameters were measured and not adjusted. The agreement between the experimental and simulated spectrum is very satisfying knowing that there is no adjustable parameter. The spectrum exhibits a discontinuity, particularly obvious for the upward sweep of the magnetic field. This discontinuity is a manifestation of the abrupt change from the lower α branch to the upper γ branch of the bistable system.

This example shows that bistable EPR in conductors is a good illustration of our approach to intrinsic optical bistability. It justifies the use of the effective spin to describe each subsystem and the factorization operation, which is based on the critical condition $\tau_c \ll \hbar/A$.

B. In the infrared and visible range: The intrinsic optical bistability of ytterbium ion pairs in $CsCdBr_3$

Hehlen *et al.* reported the first observation of a bistable phenomenon in 1% ytterbium doped $CsCdBr_3$ matrix.[11] The near-infrared luminescence and the visible cooperative emission of ytterbium ion pairs exhibit a hysteresis loop as a function of the incident power of the laser. The width of the hysteresis is obtained for excitation densities varying from about 4000 W cm^{-2} to about 6000 W cm^{-2} at low temperature (7 K) and at an excitation frequency of 10 602.8 cm^{-1}.[11] In this bromide host, the rare-earth ions form exclusively charge-compensated ion-pair centers even at low dopant concentration. The main rare-earth center is a symmetric Yb^{3+}-V_{Cd}-Yb^{3+} pair with an Yb^{3+}-Yb^{3+} distance of 5.88 Å,[44,45] V_{Cd} represents a Cd^{2+} vacancy. Asymmetric Yb^{3+}-Yb^{3+}-V_{Cd} pairs with a side vacancy and an Yb^{3+}-Yb^{3+} distance of 3.4 Å are also postulated as minor centers in $CsCdBr_3$. Only the asymmetric pairs, corresponding to the transition centered at 10 602.8 cm^{-1} with a width (full width at half maximum) equal to 0.6 cm^{-1}, give an hysteresis loop up to 16.3 K.[11] Previous studies have shown that the asymmetric pairs are not thermodynamically stable and transform, even at room temperature, into the symmetric center.[46]

As in this host, the rare-earth ions exclusively form ion pairs, it offers the opportunity to test our approach for intrinsic optical bistability in the near-infrared or visible range in the case of atomic pairs. In the following we show that the phase diagram of Fig. 7 predicts a bistable phenomenon only for the asymmetric pairs and that the experimental results obtained by Hehlen *et al.*[11] and the shape of the excitation spectra obtained by Gamelin, Lüthi, and Güdel[10] can be reproduced. The two subsystems K and L are the two Yb^{3+}

ions of the pairs. For symmetric pairs, the two subsystems are identical and for asymmetric pairs they are different. EPR spectroscopy shows that the two Yb^{3+} ions involved in symmetric pairs exhibit a very weak antiferromagnetic exchange interaction $J=-1.6\times10^{-3}$ cm^{-1}. If we report this value in the phase diagram of Fig. 7 (*s*-Yb pair), we remark that the bistable domain is very small for this symmetrical center. To observe a bistability for the symmetric pairs, one needs a homogeneous linewidth smaller than 8×10^{-4} cm^{-1}, which appears unlikely. The asymmetric pairs could not be observed by EPR.[44] However it is possible to obtain the order of magnitude of the interaction between the two ytterbium ions in such pairs. Indeed, in another bromide host $Cs_3Lu_2Br_9$, an antiferromagnetic exchange interaction J of -1.43 cm^{-1} for pairs of ytterbium ions separated by a distance of 3.8 Å has been measured by neutron spectroscopy.[47] Moreover, the existence of ferromagnetically coupled pairs of Nd^{3+} ions in neodymium doped YVO_4 matrices, with exchange coupling values J in the range $+4.9$ cm^{-1} to $+0.8$ cm^{-1} for Nd-Nd distances of 3.72–6.36 Å, has recently been shown.[39] As the Yb^{3+}-Yb^{3+} distance in the asymmetric pair is equal to 3.4 Å, we estimate the exchange interaction to be in the range 1 to 3 cm^{-1}. If we report this range of values in the phase diagram (*a*-Yb pair in Fig. 7), there is a large domain where the asymmetric pair should be able to exhibit a hysteresis phenomenon. The homogeneous linewidth associated with the transitions of asymmetric pairs should be lesser than 0.5 cm^{-1} in the case of $|\Delta\omega_L^{\max}|=1$ cm^{-1} and lesser than 1.5 cm^{-1} for $|\Delta\omega_L^{\max}|=3$ cm^{-1}. The linewidth of the transition associated with the asymmetric pairs is equal to 0.6 cm^{-1}.[11] This value gives a higher limit for T_2^L, as probably an important inhomogeneous broadening contributes to the total 0.6 cm^{-1} width of this transition. If we consider a mean value of $|\Delta\omega_L^{\max}|=2$ cm^{-1} and a homogeneous linewidth $\Gamma_h=0.6$ cm^{-1}, the phase diagram predicts a bistable behavior for the asymmetric ytterbium pairs in $CsCdBr_3$. As a conclusion, based on the values of the exchange interaction measured by EPR spectroscopy for symmetric pairs and deduced from other compounds for asymmetric pairs, the phase diagram of Fig. 7 predicts the absence of bistable behavior for symmetric pairs and a possible bistability for asymmetric pairs. These predictions are in total agreement with the results obtained by Hehlen *et al.*, where only the asymmetric pairs exhibit a bistability at low temperature.[11] It is important to remember that the phase diagram for bistability considers a fluctuating interaction with the condition $\tau_c \ll \hbar/|J|$. In this discussion we assume that this condition is fulfilled. In the case of rare-earth ions in solids, the fluctuation of the ion-ion interaction could be due to the ion-phonon interaction. Indeed, these two kind of interactions (ion-ion and ion-phonon) are competing mechanisms and the ion-phonon interaction could play an equivalent role as the motional narrowing of the EPR signal in semiconductors.

To determine if the spin-Hamiltonian approach can reproduce in more detail the bistable phenomenon observed for the asymmetric ytterbium pairs in $CsCdBr_3$, the bistable transitions are simulated in Figs. 9(a) and 9(b) by using the coupled equations (40) and (41). The parameters of the simulations are $T_1^L=7.8\times10^{-4}$ s,[48] $\Delta\omega_L^{\max}=-2$ cm^{-1}, and $T_2^L=1.77\times10^{-11}$ s (corresponding to $\Gamma_h=0.6$ cm^{-1}), which gives $|\Delta\omega_L^{\max}|T_2^L=6.6$. The abscissa scale in Fig. 9(a) is calibrated by transforming the Ω_1^2 parameter of Eq. (40) into the incident power P expressed in W cm^{-2} by using Eq. (51) with $\hbar\omega_L=10\,600$ cm^{-1}. Usually ytterbium ions exhibit oscillator strengths F_{ab} of around 10^{-6}. In the simulations, we take values of F_{ab} that vary from 10^{-7} to 10^{-6}. For an oscillator strength of 10^{-7} the simulation reproduces the order of magnitude of the incident power P obtained by Hehlen *et al.*,[11] where the hysteresis is observed for excitation densities varying from about 4000 W cm^{-1} to about 6000 W cm^{-2} at a low temperature (7 K). For an oscillator strength of 10^{-6} the simulation is still good with only an order of magnitude of discrepancy for the excitation between the experimental and the simulated hysteresis. The shape of the transition can be also simulated for different powers of the incident laser. In Fig. 9(b), we consider an oscillator strength of 10^{-7}. As the power increases, the distortion of

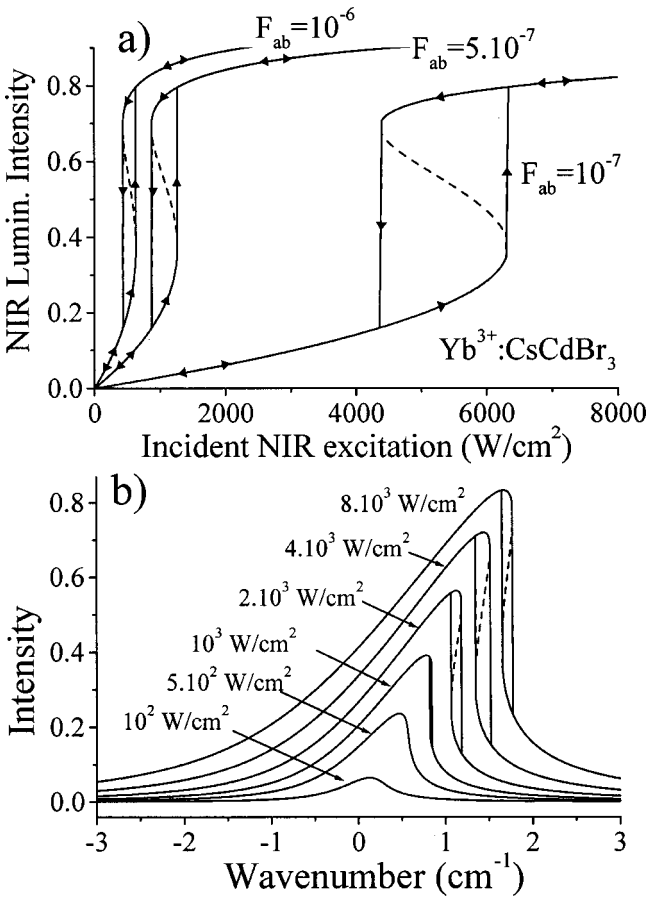

FIG. 9. (a) Simulation of the bistable infrared luminescence of asymmetric ytterbium pairs in $CsCdBr_3$. The parameters of the simulation are $T_1^L=7.8\times10^{-4}$ s, $\Delta\omega_L^{\max}=-2$ cm^{-1}, $T_2^L=1.77\times10^{-11}$ s corresponding to $\Gamma_h=0.6$ cm^{-1}, $|\Delta\omega_L^{\max}|T_2^L=6.6$. The abscissa position of the hysteresis loop is determined by taking three different values for the oscillator strength of the transition: $F_{ab}=10^{-7}$, 5×10^{-7}, 10^{-6}. (b) Simulated shape of the absorption or excitation spectra associated with the asymmetric ytterbium pairs in $CsCdBr_3$ for different values of the incident laser power.

the shape increases and an abrupt change in intensity appears on the high-energy side of the transition. As we have already seen, this behavior is associated with the switch between the two steady states of the hysteresis loop. This type of a line shape has been already observed by Gamelin, Lüthi, and Güdel in the excitation spectra of Yb^{3+}: $CsCdBr_3$.[10]

It thus appears that the theoretical approach presented in this work is able to explain qualitatively all the results obtained for the asymmetric pairs of ytterbium ions in $CsCdBr_3$. The phase diagram predicts only a bistable phenomenon for these kind of centers. By taking experimental values for T_1^L, a high limit for T_2^L, considering $\Delta\omega_L^{\max} = -2\ \mathrm{cm}^{-1}$, and an oscillator strength F_{ab} of 10^{-7}, the simulations reproduce the order of magnitude of the incident power P, which gives the hysteresis loop in the fluorescence intensity as well as the observed shape of the bistable transition.

V. CONCLUSION

A general condition for intrinsic optical bistability is studied for a system S composed of two weakly interacting subsystems that can be embedded in a medium such as a solid matrix. The important point is that the interaction V between the two subsystems must fluctuate with a correlation time $\tau_c \ll \hbar/V$. Under this condition the total density-matrix operator of the system can be factorized into two partial density operators linked to the two subsystems. During the time scale of the evolution of these subsystems, the contribution of the correlation terms can be neglected. All the approximations done in this approach have been justified by this condition. The consequence of these rapid fluctuations is that this ''factorization operation'' leads to a renormalization (a shift) of the resonance frequency of the optical transition. It means that the frequency changes continuously during the interaction with the external field.

All the systems that are described in such way can, in principle, exhibit a bistable behavior under the condition $|\Delta\omega_L^{\max}| > 2\Gamma_h$, which means that the maximum shift of the frequency has to be larger than the homogeneous linewidth of the transition. Under this condition, there is at least one value of the external control parameter that gives a bistable response of the system. It is important to notice that when the system is set under bistable conditions, all the control parameters, such as the temperature T, the frequency ω, and the incident power P of the external electromagnetic field, can produce a bistable phenomenon. The condition $|\Delta\omega_L^{\max}| > 2\Gamma_h$ can be visualized by a phase diagram that determines the conditions for a system to exhibit a bistable response under a sweep of an external control parameter. This phase diagram seems to accurately predict the systems that could exhibit an intrinsic spectroscopic bistability.

In the microwave range corresponding to EPR spectroscopy, all the compounds (β-Ga_2O_3, metallic lithium, and InP) that are placed in the bistable domain of the phase diagram have revealed an experimental intrinsic bistability in the microwave (EPR) range. In this case the feedback loop originates from the Overhauser effect.

In the near-infrared and visible range, we have shown that a pair of ions can exhibit a bistable behavior. However, the dipole-dipole interaction, which is at the origin of the Lorentz local-field correction, seems too small to be at the origin of the experimental bistability. An interaction V of a few cm^{-1}, such as an exchange-type interaction, is required. In the particular case of two identical ions in scalar interaction, the shift of the resonance vanishes and the phenomenon cannot exist. The phase diagram predicts the absence and the existence of a bistable luminescence of the symmetric and asymmetric ytterbium pairs in $CsCdBr_3$, respectively. IOB has been experimentally demonstrated in this compound by Helhen *et al.*,[11] and the simulations performed with our approach reproduce the bistable response versus incident laser power as well as the shape of the excitation spectra.[10]

Finally, the effects of the material-dependent parameters, which are the longitudinal and transverse relaxation terms T_1^L and T_2^L and the leakage factor f_L, have been studied. The system will exhibit IOB if (i) the homogeneous transition linewidth is very small implying a long transverse relaxation time T_2^L, (ii) the leakage factor f_L is strong enough to give a good efficiency of the polarization transfer between the two subsystems, and (iii) the longitudinal relaxation T_1^L is sufficiently long to obtain a moderate saturability of the transition at a rather low incident power.

The results presented in this work are only preliminary concerning the infrared and visible range. Several points must be developed and several questions have to be answered to expect to find a compound that will exhibit IOB at ambient temperature: (i) How can we control the magnitude of the interaction between the two ions involved in the pairs and the material-dependent parameters in terms of a structure-properties relationship? (ii) What are the mechanisms responsible for the fluctuating interaction, allowing the condition $\tau_c \ll \hbar/V$ to be fulfilled? (iii) Is it possible to obtain such a bistable phenomenon for other kind of interacting subsystems? All these studies are currently in progress.

ACKNOWLEDGMENTS

The authors thank Dr. Ph. Goldner for fruitful discussions. Laboratoire de Chimie Appliquée de l'Etat Solide is Unité Mixte de Recherche of the Center National de la Recherche Scientifique (CNRS) No. 7574.

APPENDIX: CALCULATIONS OF THE KINETIC EQUATIONS

Let us consider a system S composed of two subsystems K and L with a weak interaction V. Under the condition $\tau_c \ll \hbar/V$ and for an integration time Δt characterized by $\tau_c \ll \Delta t \ll T_{1,2}^{L\,\mathrm{int}}, T_{1,2}^{K\,\mathrm{int}}$, the kinetic equation associated with the quantum-mechanical average of an operator Q is given by

$$\frac{d\langle Q\rangle}{dt} = -\frac{1}{i\hbar}\left\langle\left[H_K + H_L + \sum_p \left(\langle F_p\rangle S^{(p)} + \langle F_p^*\rangle S^{(p^+)}\right), Q\right]\right\rangle - \frac{1}{2\hbar^2}\sum_p J_{pp^+}(\omega^{S^{(p)}})\left\langle\left[S^{(p^+)}, [S^{(p)}, Q - Q^0]\right]\right\rangle, \tag{A1}$$

where we only take into account the secular terms and where we have neglected imaginary terms responsible for a second-order shift of the resonance, which are usually too small to be detected.

If we consider the general form of the interaction V given by Eq. (8), Eq. (A1) can be written in the form

$$\frac{d\langle Q\rangle}{dt}=-\frac{1}{i\hbar}\left\langle\left[\hbar\omega_L L_z+\hbar\omega_K K_z+\sum_p\ (\langle F_p\rangle S^{(p)}+\langle F_p^*\rangle S^{(p+)}),Q\right]\right\rangle-\frac{1}{2\hbar^2}J_{00}(0)\langle[L_zK_z,[L_zK_z,Q-Q^0]]\rangle-\frac{1}{2\hbar^2}J_{11*}(\omega_K-\omega_L)\times\begin{pmatrix}\langle[L_+K_-,[L_-K_+,Q-Q^0]]\rangle\\+\langle[L_-K_+,[L_+K_-,Q-Q^0]]\rangle\end{pmatrix}-\frac{1}{2\hbar^2}J_{22*}(\omega_L)\times\begin{pmatrix}\langle[L_-K_z,[L_+K_z,Q-Q^0]]\rangle\\+\langle[L_+K_z,[L_-K_z,Q-Q^0]]\rangle\end{pmatrix}-\frac{1}{2\hbar^2}J_{33*}(\omega_K)\times\begin{pmatrix}\langle[L_zK_+,[L_zK_-,Q-Q^0]]\rangle\\+\langle[L_zK_-,[L_zK_+,Q-Q^0]]\rangle\end{pmatrix}-\frac{1}{2\hbar^2}J_{44*}\times(\omega_K+\omega_L)\begin{pmatrix}\langle[L_-K_-,[L_+K_+,Q-Q^0]]\rangle\\+\langle[L_+K_+,[L_-K_-,Q-Q^0]]\rangle\end{pmatrix}\tag{A2}$$

with

$$J_{00}(0)=\langle|F_0|^2\rangle 2\tau_c,$$

$$J_{11*}(\omega_K-\omega_L)=\langle|F_1|^2\rangle\frac{2\tau_c}{1+(\omega_K-\omega_L)^2\tau_c^2},$$

$$J_{22*}(\omega_L)=\langle|F_2|^2\rangle\frac{2\tau_c}{1+(\omega_L)^2\tau_c^2},$$

$$J_{33*}(\omega_K)=\langle|F_3|^2\rangle\frac{2\tau_c}{1+(\omega_K)^2\tau_c^2},$$

$$J_{44*}(\omega_K+\omega_L)=\langle|F_4|^2\rangle\frac{2\tau_c}{1+(\omega_K+\omega_L)^2\tau_c^2}.$$

Two cases have to be considered in which the two subsystems K and L are different or identical.

(i) *Different L, K systems*. The following kinetic equations are obtained for $\langle L_z\rangle$, $\langle L_+\rangle$:

$$\frac{d\langle L_z\rangle}{dt}=i\frac{\langle F_1\rangle}{\hbar}(\langle L_-\rangle\langle K_+\rangle-\langle L_+\rangle\langle K_-\rangle)+i\frac{\langle F_2\rangle}{\hbar}(\langle L_-\rangle\langle K_z\rangle-\langle L_+\rangle\langle K_z\rangle)+i\frac{\langle F_4\rangle}{\hbar}(\langle L_-\rangle\langle K_-\rangle-\langle L_+\rangle\langle K_+\rangle)-\frac{3}{4}\frac{1}{T_1^{LL}}(\langle L_z\rangle-\langle L_z\rangle^0)+\frac{3}{4}\frac{1}{T_1^{LK}}(\langle K_z\rangle-\langle K_z\rangle^0),\tag{A3}$$

$$\frac{d\langle L_+\rangle}{dt}=i\left(\omega_L+\frac{\langle F_0\rangle}{\hbar}\langle K_z\rangle\right)\langle L_+\rangle-2i\frac{\langle F_1\rangle}{\hbar}\langle L_z\rangle\langle K_+\rangle-2i\frac{\langle F_2\rangle}{\hbar}\langle L_z\rangle\langle K_z\rangle-2i\frac{\langle F_4\rangle}{\hbar}\langle L_z\rangle\langle K_-\rangle+i\frac{\langle F_3\rangle}{\hbar}(\langle L_+\rangle\langle K_+\rangle+\langle L_+\rangle\langle K_-\rangle)-\frac{1}{T_2^{L\,\mathrm{int}}}\langle L_+\rangle\tag{A4}$$

with $\langle L_\pm\rangle^0=0$, $\langle K_\pm\rangle^0=0$ and

$$\frac{1}{T_1^{LL}}=\frac{8}{3\hbar^2}\langle|F_1|^2\rangle\frac{\tau_c}{1+(\omega_K-\omega_L)^2\tau_c^2}+\frac{4}{3\hbar^2}\langle|F_2|^2\rangle\frac{\tau_c}{1+(\omega_L)^2\tau_c^2}+\frac{8}{3\hbar^2}\langle|F_4|^2\rangle\frac{\tau_c}{1+(\omega_K+\omega_L)^2\tau_c^2},\tag{A5}$$

$$\frac{1}{T_1^{LK}}=+\frac{8}{3\hbar^2}\langle|F_1|^2\rangle\frac{\tau_c}{1+(\omega_K-\omega_L)^2\tau_c^2}-\frac{8}{3\hbar^2}\langle|F_4|^2\rangle\frac{\tau_c}{1+(\omega_K+\omega_L)^2\tau_c^2},\tag{A6}$$

$$\frac{1}{T_2^{L\,\mathrm{int}}}=+\frac{1}{3\hbar^2}\langle|F_0|^2\rangle\tau_c+\frac{4}{3\hbar^2}\langle|F_1|^2\rangle\frac{\tau_c}{1+(\omega_K-\omega_L)^2\tau_c^2}+\frac{2}{3\hbar^2}\langle|F_2|^2\rangle\frac{\tau_c}{1+(\omega_L)^2\tau_c^2}+\frac{4}{3\hbar^2}\langle|F_3|^2\rangle\frac{\tau_c}{1+(\omega_K)^2\tau_c^2}+\frac{4}{3\hbar^2}\langle|F_4|^2\rangle\frac{\tau_c}{1+(\omega_K+\omega_L)^2\tau_c^2}.\tag{A7}$$

For $\langle K_z\rangle$, $\langle K_+\rangle$, we have

$$\frac{d\langle K_z\rangle}{dt}=+i\frac{\langle F_1\rangle}{\hbar}(\langle K_-\rangle\langle L_+\rangle-\langle K_+\rangle\langle L_-\rangle)+i\frac{\langle F_3\rangle}{\hbar}(\langle K_-\rangle\times\langle L_z\rangle-\langle K_+\rangle\langle L_z\rangle)+i\frac{\langle F_4\rangle}{\hbar}(\langle K_-\rangle\langle L_-\rangle-\langle K_+\rangle\times\langle L_+\rangle)-\frac{3}{4}\frac{1}{T_1^{KK}}(\langle K_z\rangle-\langle K_z\rangle^0)+\frac{3}{4}\frac{1}{T_1^{LK}}(\langle L_z\rangle-\langle L_z\rangle^0),\tag{A8}$$

$$\frac{d\langle K_+\rangle}{dt} = i\left(\omega_K + \frac{\langle F_0\rangle}{\hbar}\langle L_z\rangle\right)\langle K_+\rangle - 2i\frac{\langle F_1\rangle}{\hbar}\langle K_z\rangle\langle L_+\rangle - 2i\frac{\langle F_3\rangle}{\hbar}\langle K_z\rangle\langle L_z\rangle - 2i\frac{\langle F_4\rangle}{\hbar}\langle K_z\rangle\langle L_-\rangle + i\frac{\langle F_2\rangle}{\hbar}(\langle K_+\rangle\langle L_+\rangle + \langle K_+\rangle\langle L_-\rangle) - \frac{1}{T_2^{K\,\mathrm{int}}}\langle K_+\rangle \tag{A9}$$

with

$$\frac{1}{T_1^{KK}} = \frac{8}{3\hbar^2}\langle|F_1|^2\rangle\frac{\tau_c}{1+(\omega_K-\omega_L)^2\tau_c^2} + \frac{4}{3\hbar^2}\langle|F_3|^2\rangle\frac{\tau_c}{1+(\omega_K)^2\tau_c^2} + \frac{8}{3\hbar^2}\langle|F_4|^2\rangle\frac{\tau_c}{1+(\omega_K+\omega_L)^2\tau_c^2}, \tag{A10}$$

$$\frac{1}{T_2^{K\,\mathrm{int}}} = +\frac{1}{3\hbar^2}\langle|F_0|^2\rangle\tau_c + \frac{4}{3\hbar^2}\langle|F_1|^2\rangle\frac{\tau_c}{1+(\omega_K-\omega_L)^2\tau_c^2} + \frac{4}{3\hbar^2}\langle|F_2|^2\rangle\frac{\tau_c}{1+(\omega_L)^2\tau_c^2} + \frac{2}{3\hbar^2}\langle|F_3|^2\rangle\frac{\tau_c}{1+(\omega_K)^2\tau_c^2} + \frac{4}{3\hbar^2}\langle|F_4|^2\rangle\frac{\tau_c}{1+(\omega_K+\omega_L)^2\tau_c^2}. \tag{A11}$$

The above equations are obtained by using the well-known commutation rules between the different operators L_z, L_+, L_-, by using the condition $\tau_c \ll \hbar/V$, which allows us to write $\sigma^S = \sigma^K \otimes \sigma^L$ and then $\langle L^{(p)}K^{(p)}\rangle = \langle L^{(p)}\rangle\langle K^{(p)}\rangle$, and by considering $\langle L_z^2\rangle = L(L+1)/3 = \frac{1}{4}$, $\langle L^2\rangle = L(L+1) = \frac{3}{4}$. By applying an external field (magnetic or electric) with ω its angular frequency under the condition $\tau_c \ll \Omega_1^{-1}$, where Ω_1 is the Rabi frequency, we can add to the above kinetic equations the contribution of the Hamiltonian representing the interaction between the external field and the system. In the case of an electric field, the Rabi frequency is $\Omega_1 = d\xi/\hbar$, where d is the electric dipole moment and ξ is the amplitude of the electric field in the slowly varying envelope approximation ($\dot{\xi}/\xi = 0$). If we consider, for example, a transition on the effective spin L and other relaxation mechanisms represented by $T_{1,2}^{L\,\mathrm{other}}$, $T_{1,2}^{K\,\mathrm{other}}$, which follow the usual Bloch equations, the equations (A3), (A4), (A8), and (A9) written in the quasiresonant approximation $|\omega-\omega_L| \ll \omega_L$, the slowly varying envelope approximation, and the rotating coordinate system become

$$\frac{d\langle L_z\rangle}{dt} = -\frac{3}{4}\frac{1}{T_1^{LL}}(\langle L_z\rangle - \langle L_z\rangle^0) + \frac{3}{4}\frac{1}{T_1^{LK}}(\langle K_z\rangle - \langle K_z\rangle^0) - \frac{1}{T_1^{L\,\mathrm{other}}}(\langle L_z\rangle - \langle L_z\rangle^0) + \frac{i\Omega_1}{2}(\langle L'_-\rangle - \langle L'_+\rangle), \tag{A12}$$

$$\frac{d\langle L'_+\rangle}{dt} = +i\left(\omega_L - \omega + \frac{\langle F_0\rangle}{\hbar}\langle K_z\rangle\right)\langle L'_+\rangle - \frac{1}{T_2^L}\langle L'_+\rangle - i\Omega_1\langle L_z\rangle \tag{A13}$$

with $1/T_2^L = 1/T_2^{L\,\mathrm{int}} + 1/T_2^{L\,\mathrm{other}}$,

$$\frac{d\langle K_z\rangle}{dt} = -\frac{3}{4}\frac{1}{T_1^{KK}}(\langle K_z\rangle - \langle K_z\rangle^0) + \frac{3}{4}\frac{1}{T_1^{LK}}(\langle L_z\rangle - \langle L_z\rangle^0) - \frac{1}{T_1^{K\,\mathrm{other}}}(\langle K_z\rangle - \langle K_z\rangle^0), \tag{A14}$$

$$\frac{d\langle K'_+\rangle}{dt} = 0, \tag{A15}$$

where $L'_\pm = L_\pm e^{\pm i\omega t}$. We obtain similar kinetic equations if we apply the external field to the K system.

A lot of terms have been neglected in Eqs. (A12)–(A15). Indeed, near the resonance ($\omega \sim \omega_L$) and in the sense of the slowly varying envelope approximation, the dominant contribution to the above relaxation equations originates from the low-frequency terms in $e^{\pm i(\omega-\omega_L)t}$ as $\langle L_-\rangle$, $\langle L_+\rangle$. The contributions of $\langle K_\mp\rangle\langle L_\pm\rangle$, $\langle K_\mp\rangle\langle L_\mp\rangle$, $\langle K_z\rangle\langle L_\pm\rangle$, and $\langle K_\pm\rangle\langle L_z\rangle$ can be neglected because they correspond to high-frequency terms in $e^{\pm i(\omega_L-\omega_K)t}$, $e^{\pm i(\omega_L+\omega_K)t}$, $e^{\pm i(\omega_L)t}$, and $e^{\pm i(\omega_K)t}$, respectively.

(ii) *Identical L, K systems*. In the case of two identical ions, the rotating coordinate system, the quasiresonant approximation $|\omega-\omega_L| \ll \omega_L$, and the slowly varying envelope approximation give the following set of kinetic equations:

$$\frac{d\langle L_z\rangle}{dt} = -\frac{1}{T_1^L}(\langle L_z\rangle - \langle L_z\rangle^0) + i\frac{\Omega_1}{2}(\langle L'_-\rangle - \langle L'_+\rangle), \tag{A16}$$

$$\frac{d\langle L'_+\rangle}{dt} = i\left[\omega_L - \omega + \left(\frac{\langle F_0\rangle}{\hbar} - 2\frac{\langle F_1\rangle}{\hbar}\right)\langle L_z\rangle\right]\langle L'_+\rangle - \frac{1}{T_2^L}\langle L'_+\rangle - i\Omega_1\langle L'_z\rangle \tag{A17}$$

with

$$\frac{1}{T_1^L} = -\frac{3}{4}\left(\frac{1}{T_1^{LK}} - \frac{1}{T_1^{LL}}\right) + \frac{1}{T_1^{L\,\mathrm{other}}} \tag{A18}$$

and

$$\frac{1}{T_2^L} = \frac{1}{T_2^{L\,\mathrm{int}}} + \frac{1}{T_2^{L\,\mathrm{other}}}. \tag{A19}$$

*Author to whom correspondence should be addressed. Electronic address: guillotn@ext.jussieu.fr

[1] P. Mandel, S. D. Smith, and B. S. Wherrett, *From Optical Bistability Towards Optical Computing*, (Elsevier, The Netherlands, 1987); E. Abraham and S. D. Smith, Rep. Prog. Phys. **45**, 138 (1982).

[2] A. E. Kaplan, Phys. Rev. Lett. **48**, 138 (1982); G. Gabrielse, H. Dehmelt, and W. Kells, *ibid.* **54**, 537 (1985); A. E. Kaplan and A. Elci, Phys. Rev. B **29**, 820 (1984).

[3] E. Aubay and D. Gourier, J. Phys. Chem. **96**, 5513 (1992); Phys. Rev. B **47**, 15023 (1993); D. Gourier, E. Aubay, and J. Guglielmi, *ibid.* **50**, 2941 (1994); D. Gerbault and D. Gourier, *ibid.* **54**, 6315 (1996); **57**, 2679 (1998); D. Gourier, L. Binet, and D. Gerbaut, Appl. Magn. Reson. **14**, 183 (1998).

[4] L. Binet and D. Gourier, Phys. Rev. B **56**, 2688 (1997).

[5] C. Vigreux, L. Binet, and D. Gourier, J. Phys. Chem. B **102**, 1176 (1998); C. Vigreux, P. Loiseau, L. Binet, and D. Gourier, Phys. Rev. B **61**, 8759 (2000).

[6] K. Bohnert, H. Kalt, and C. Klingshirn, Appl. Phys. Lett. **43**, 1088 (1983); M. Dagenais and W. F. Sharfin, *ibid.* **45**, 210 (1984); R. Neuendorf, M. Quinten, and U. Kreiberg, J. Chem. Phys. **104**, 6348 (1996).

[7] A. Overhauser, Phys. Rev. **92**, 411 (1953).

[8] M. P. Hehlen, H. U. Güdel, Q. Shu, J. Rai, S. Rai, and S. C. Rand, Phys. Rev. Lett. **73**, 1103 (1994); M. P. Hehlen, H. U. Güdel, Q. Shu, and S. C. Rand, J. Chem. Phys. **104**, 1232 (1996).

[9] S. R. Lüthi, M. P. Hehlen, T. Riedener, and H. U. Güdel, J. Lumin. **76–77**, 447 (1998).

[10] D. R. Gamelin, S. R. Lüthi, and H. U. Güdel, J. Phys. Chem. B **104**, 11 045 (2000).

[11] M. P. Hehlen, A. Kuditcher, S. C. Rand, and S. R. Lüthi, Phys. Rev. Lett. **82**, 3050 (1999).

[12] A. Kuditcher, M. P. Hehlen, C. M. Florea, K. W. Winick, and S. C. Rand, Phys. Rev. Lett. **84**, 1898 (2000).

[13] C. M. Bowden and C. Sung, Phys. Rev. A **19**, 2392 (1979); C. M. Bowden, A. Postan, and R. Inguva, J. Opt. Soc. Am. B **8**, 1081 (1991); C. M. Bowden and J. P. Dowling, Phys. Rev. A **47**, 1247 (1993).

[14] C. M. Bowden and M. E. Crenshaw, Opt. Commun. **179**, 63 (2000).

[15] F. A. Hopf, C. M. Bowden, and W. H. Louisell, Phys. Rev. A **29**, 2591 (1984); F. A. Hopf and C. M. Bowden, *ibid.* **32**, 268 (1985).

[16] R. Friedberg, S. R. Hartmann, and J. T. Manassah, Phys. Rev. A **40**, 2446 (1989).

[17] Y. Ben-Aryeh and C. M. Bowden, Opt. Commun. **59**, 224 (1986); Y. Ben-Aryeh, C. M. Bowden, and J. C. Englund, Phys. Rev. A **34**, 3917 (1986).

[18] C. R. Stroud, C. M. Bowden, and L. Allen, Opt. Commun. **67**, 387 (1988).

[19] R. Inguva and C. M. Bowden, Phys. Rev. A **41**, 1670 (1990).

[20] M. E. Crenshaw, M. Scalora, and C. M. Bowden, Phys. Rev. Lett. **68**, 911 (1992); M. E. Crenshaw and C. M. Bowden, Phys. Rev. A **53**, 1139 (1996); M. E. Crenshaw, *ibid.* **54**, 3559 (1996).

[21] J. Heber, Z. Phys. B: Condens. Matter **68**, 115 (1987); N. Bodenschatz and J. Heber, Phys. Rev. A **54**, 4428 (1996); J. Heber, J. Alloys Compd. **300–301**, 32 (2000).

[22] V. A. Malyshev, H. Glaeske, and K. H. Feller, Phys. Rev. A **58**, 1496 (1998).

[23] V. A. Malyshev and P. Moreno, Phys. Rev. A **53**, 416 (1996); V. A. Malyshev, H. Glaeske, and K. H. Feller, J. Lumin. **76–77**, 455 (1998); Opt. Commun. **169**, 177 (1999); J. Lumin. **83–84**, 191 (1999); V. A. Malyshev and E. C. Jarque, Opt. Express **6**, 227 (2000); V. A. Malyshev, H. Glaeske, and K. H. Feller, J. Chem. Phys. **113**, 1170 (2000); H. Glaeske, V. A. Malyshev, and K. H. Feller, *ibid.* **114**, 1966 (2001).

[24] A. Abragam, *Principles of Nuclear Magnetism* (Clarendon, Oxford, 1983).

[25] I. Solomon, Phys. Rev. **99**, 559 (1955).

[26] C. Cohen-Tannoudji, J. Dupont-Roc, and G. Grynberg, *Processus d'Interaction entre Photons et Atomes* (Intereditions/Edition du CNRS, Paris, 1988).

[27] K. Blum, *Density Matrix Theory and Applications*, Physics of Atoms and Molecules (Plenum Press, New York, 1981).

[28] N. M. Atherton, *Electron Spin Resonance*, Theory and Applications (Wiley, New York, 1973).

[29] M. Nechstein, F. Devreux, F. Genoud, M. Guglielmi, and H. Holczer, Phys. Rev. B **27**, 61 (1983); G. Denninger, W. Stöcklein, E. Dormann, and M. Schwoerer, Chem. Phys. Lett. **107**, 222 (1984); W. Stöcklein and G. Denninger, Mol. Cryst. Liq. Cryst. **136**, 335 (1986); H. Brunner, K. Hauser, H. J. Keller, and D. Schweitzer, Solid State Commun. **51**, 107 (1984).

[30] D. Paget, G. Lampel, B. Sapoval, and V. I. Safarov, Phys. Rev. B **15**, 5780 (1977).

[31] D. Gourier, L. Binet, and E. Aubay, J. Chem. Phys. **92**, 1831 (1995); E. Aubay and D. Gourier, Solid State Commun. **85**, 821 (1993).

[32] C. R. Carver and C. P. Slichter, Phys. Rev. **102**, 975 (1956).

[33] M. Gueron and C. Ryter, Phys. Rev. Lett. **3**, 338 (1959); C. Ryter, Phys. Rev. **5**, 10 (1960).

[34] B. Gothschi, G. Denninger, H. Obloh, W. Wilkening, and J. Schneider, Solid State Commun. **71**, 629 (1989); B. Clerjaud, F. Gendron, H. Obloh, J. Schneider, and W. Wilkening, Phys. Rev. B **40**, 2042 (1989).

[35] R. L. Cone and R. S. Meltzer, *Spectroscopy of Solids Containing Rare Earth Ions*, Modern Problems in Condensed Matter Science Vol. 21 (North-Holland, Amsterdam, 1987), Chap. 8, p. 481.

[36] M. J. Berggren, G. F. Imbusch, and P. L. Scott, Phys. Rev. **188**, 675 (1969).

[37] R. M. Macfarlane and R. M. Shelby, *Spectroscopy of Solids Containing Rare Earth Ions*, (Ref. 35), Chap. 3, p. 51.

[38] E. P. Chukalina, M. N. Popova, S. L. Korableva, and R. Y. Abdulsabirov, Phys. Lett. A **269**, 348 (2000).

[39] O. Guillot-Noël, V. Mehta, B. Viana, D. Gourier, M. Boukhris, and S. Jandl, Phys. Rev. B **61**, 15 338 (2000).

[40] T. T. Basiev, V. V. Fedorov, A. Y. Karasik, and K. K. Pukhov, J. Lumin. **81**, 189 (1999).

[41] M. P. Hehlen and H. U. Güdel, J. Chem. Phys. **98**, 1768 (1993).

[42] O. Guillot-Noël, B. Bellamy, B. Viana, and D. Gourier, Phys. Rev. B **60**, 1668 (1999).

[43] Y. Y. Perlin, A. A. Kaminskii, S. I. Klokishner, V. N. Enakii, Kh. S. Bagdasarov, G. A. Bogomolova, and D. N. Vylegzhanin, Phys. Status Solidi A **40**, 643 (1977).

[44] V. Mehta and D. Gourier, J. Phys.: Condens. Matter **13**, 4567 (2001).

[45] G. L. McPherson and L. M. Henling, Phys. Rev. B **16**, 1889

(1977); L. M. Henling and G. L. Mcpherson, *ibid.* **16**, 4756 (1977).
[46] J. Heber, U. Schäfer, J. Neukum, and N. Bodenschatz, Acta Phys. Pol. A **84**, 889 (1993).
[47] H. U. Güdel, A. Furrer, and H. Blank, Inorg. Chem. **29**, 4081 (1990).
[48] Ph. Goldner, F. Pellé, D. Meichenin, and F. Auzel, J. Lumin. **71**, 137 (1997).